

ABSTRACT

Title of Document ALTERNATIVE DYNAMIC TESTING BY
ACTIVE CONTROL

Nicholas Alexander Wagman,
Master of Science, 2012

Directed by: Professor Peter Chang, Department of Civil and
Environmental Engineering

As the general public becomes increasingly aware of the seismic risk to structures, Americans expect assurance from structural engineering professionals that building designs are safe and reliable. Increasing public scrutiny places even greater emphasis on the need for research and validation of performance-based earthquake engineering designs. Current methods for experimental validation of designs with full-scale tests (e.g. shake table and pseudo dynamic testing) can be extremely expensive and the facilities necessary are not available at many universities. This thesis proposes an Alternative Dynamic Test which uses a properly scaled model test specimen and a desktop shake table to perform accurate experimental validation of structural designs. The methodology and laboratory setup of this testing method are discussed including the motor characterization and power requirements. Error approximation and practical implementation of the Alternative Dynamic Test are also addressed.

ALTERNATIVE DYNAMIC TESTING BY ACTIVE CONTROL

By

Nicholas Alexander Wagman

Thesis submitted to the Faculty of the Graduate School of the
University of Maryland, College Park, in partial fulfillment
of the requirements for the degree of
Master of Science
2012

Advisory Committee:
Professor Peter Chang, Chair
Professor M. Sherif Aggour
Professor Yunfeng Zhang

© Copyright by
Nicholas Alexander Wagman
2012

Dedication

This work is dedicated to my family for their love and support throughout my life and for always encouraging me to excel and pursue excellence.



A.I.D.G.

Acknowledgements

The research performed in this thesis was supported and funded by the
Department of Civil and Environmental Engineering

My graduate fellowship was funded through the United States Department of
Defense SMART Fellowship.

Many thanks to my advisor Dr. Peter Chang for his insight, guidance, and support
throughout my education at the University of Maryland and for providing me this
research opportunity.

Special thanks to Mac Roberts of Eagle Engineering for his technical support
throughout the project and volunteering his time to get the linear encoder and
motor operational. Your support has been invaluable and I cannot thank you
enough for your time and assistance.

Special thanks to Jay Renner, the Lab Manager of the BAE Controls Lab in the
Kim Engineering Building for providing abundant lab space and generous
technical support throughout the research project. I truly appreciate your
hospitality in your lab and going above and beyond to help me with my research.

Special thanks to Bryan Quinn, Joe Kselman, and their technicians in ECE Tech
Ops for designing and machining the mounting systems for the linear encoder.

Additional thanks to Glen Lichtwark from the University of Queensland,
Australia for his MATLAB code used to stream Tracking Tools data into
Simulink and to Charles Schupler for his prior work integrating the cameras and
MATLAB and his assistance in this area during my research.

Thank You!

Table of Contents

Dedication	ii
Acknowledgements	iii
List of Tables	vi
List of Figures	vii
Chapter 1: Introduction	1
1.1 Problem Statement	1
1.2 Alternative Dynamic Test	3
1.3 Active Control	5
1.4 Research Objective	6
1.5 Outline of Thesis	6
Chapter 2: Alternative Dynamic Test Methodology	8
2.1 Scale Modeling	8
2.1.1 Need for Scale Modeling in the Alternative Dynamic Test	8
2.1.2 Structural analysis of simple frame	10
2.1.3 Strength demand under earthquake load	12
2.1.4 Using scale modeling to reduce motor power requirement	14
2.2 Active Control	16
2.3 Error Approximation	17
Chapter 3: Motor Characterization	20
3.1 Motor Requirements	20
3.2 Motor Specification	20
3.3 Procedure	23
Chapter 4: Experimental Setup	28
4.1 Overview of Components	28
4.2 Linear Motor	30

4.3 Linear Encoder	32
4.4 Tracking Cameras	43
4.5 Processing.....	47
4.6 Arduino Active Control.....	51
Chapter 5: Results and Analysis	53
5.1 Commentary	53
Chapter 6: Conclusions and Future Work.....	60
6.1 Conclusions	60
6.2 Future Work	62
Bibliography	65

List of Tables

Table 1 - Comparison of motor requirements for various member materials.....	15
Table 2 - SM-S4209M servo motor specification.....	21
Table 3 - Arduino code for controlling servo motor.....	27
Table 4 - TT_Tools_demo m-file	47

List of Figures

Figure 1 - Typical steel MRF connection	4
Figure 2 - Simple frame for analysis.....	10
Figure 3 - Characteristic curve of moment-rotation relationship at plastic hinges	11
Figure 4 - 2% and 5% damped pseudo-acceleration response spectra for NR94cnp	12
Figure 5 - Scaled ground motion spectrum for NR94cnp record.....	13
Figure 6 - Error in the implementation of the control algorithm	18
Figure 7 - Servo motor and spring assembly	22
Figure 8 – Equipment setup for servo motor characterization.....	23
Figure 9 - Top down view of characterization circuitry configuration.....	24
Figure 10 - Breadboard configured for servo motor characterization	25
Figure 11 - Circuit diagram of voltage regulator	26
Figure 12 - Kollmorgen Platinum DDL (Direct Drive Linear) motor	30
Figure 13 - Kollmorgen Platinum DDL (Direct Drive Linear) motor	31
Figure 14 - Interior circuitry and layout of Newall SGH-TT encoder.....	33
Figure 15 - Newall SHG-TT Linear Encoder reader head.....	34
Figure 16 - Custom mounting plate for encoder reader head	35
Figure 17 - Newall encoder mounted via mounting plate.....	36
Figure 18 - Custom anchor block for linear encoder supports.....	37
Figure 19 - Linear encoder mounted to linear motor	38
Figure 20 - Desktop shake table.....	39
Figure 21 - Kollmorgen control box	40
Figure 22 - Screenshot of Kollmorgen Workbench software	41
Figure 23 - Desktop shake table assembly.....	42
Figure 24 - NaturalPoint OptiTrack camera	43

Figure 25 - NaturalPoint OptiTrack reflective markers (tracking spheres)	44
Figure 26 - Tracking sphere mounted in frame joint	44
Figure 27 - Tracking spheres mounted to test frame	45
Figure 28 - Experimental array of NaturalPoint OptiTrack cameras.....	46
Figure 29 - Data processing computers	50
Figure 30 - Active Control Feedback Process	51
Figure 31 - Arduino Duemilanove Microcontroller.....	52
Figure 32 - Kollmorgen linear motor with Heidenhain encoder mounted.....	54
Figure 33 - Linear motor configured in Wake and Shake mode in Kollmorgen Workbench.....	57

Chapter 1: Introduction

1.1 Problem Statement

Recent earthquakes in the Northeast United States, including the 2010 3.4-magnitude earthquake in Germantown, MD and the 5.8-magnitude Mineral, VA earthquake, which shook the entire East coast in 2011, have increased public awareness of seismic risk to structures. The issue of seismic design once seemed relegated to California and other areas of high seismic risk and activity, however with local earthquakes shaking this nation and high-magnitude earthquakes in Haiti, Chile, New Zealand, and Japan causing widespread damage worldwide people want to be certain that their homes, schools, and workplaces are safely designed to endure seismic events. This public scrutiny of designs places even greater emphasis on the need for research and validation of performance-based earthquake engineering designs.

Experimental validations of earthquake engineering designs currently include shake table and pseudo dynamic testing (PsD). Shake table testing is widely used in structural laboratories across the United States, but can be cost prohibitive because full-scale testing is extremely expensive and often impractical to perform. Furthermore, many universities do not have the infrastructure in place (e.g. strong floors, full-scale assemblies and testing apparatus) for such

experimental evaluation. In an effort to share resources for earthquake engineering research, the National Science Foundation established the national Network for Earthquake Engineering Simulation (NEES). NEES is a network of shared-use experimental research equipment sites distributed throughout the U.S. (Lehigh, Illinois, etc.) that allows for collaboration in earthquake engineering research; however, the challenges of cost and size still limit full-scale experimental testing. PsD testing was developed in 1975 by Takanashi et al as an alternative to full-scale shake table testing and has been widely used because of its versatility to test full scale structures and small scale structures, as well as substructures and subassemblies. PsD tests of lateral-load resisting systems are often used in lieu of full-scale building tests because of their lower cost compared to full-scale shake table tests. However, PsD testing is still costly to perform, and does not properly model full-scale structures due to its quasi-static nature. PsD testing fails to properly account for heat-dissipation and rate-dependent effects that may significantly influence the simulated dynamic response of earthquake systems.

The limitations of full-scale shake table and PsD tests create need for an alternative test for earthquake-resistant structures. The use of scale models with appropriate implementation of scaling laws would be a less expensive and more reliable alternative to conventional full scale tests.

1.2 Alternative Dynamic Test

The Alternative Dynamic Test offers a promising alternative to conventional full-scale testing methods for validating earthquake engineering designs. The successful development of the Alternative Dynamic Test will significantly advance earthquake engineering research by facilitating the dynamic testing of complex multi-story structures to

- (1) increase our understanding of the inelastic dynamic behavior of structures,
- (2) evaluate and quantify the seismic performance of existing systems as well as new designs, and
- (3) test the applicability of advanced materials and techniques for earthquake damage mitigation.

The core concept of the Alternative Dynamic Test is using scale models of structural systems and active control to represent the inelastic response of a structure exposed to seismic activity. Controllers provide the necessary resistance and deformation to mimic inelastic effects at specific locations in the structural system. The required inelastic response of the structure can be obtained from either a concurrent dynamic test of the substructure or an analytical model.

Structural steel moment-resisting frame (SMRF) structures, commonly used in seismic-prone areas, will be utilized to validate the seismic experimental studies. Recent earthquakes (e.g. Northridge, California in 1994 and Kobe, Japan in 1995) have demonstrated that the majority of

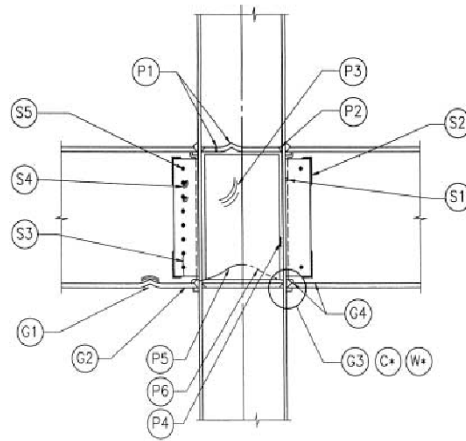


Figure 1 - Typical steel MRF connection

inelastic behavior in moment-resisting frame structures is confined to the beam-column connections. For instance, in the Northridge earthquake, fractures were present in the beam-column connection region and were nearly always initiated in or near the critical weld used to connect beam flanges to the column flange.

Based on damage from the Northridge earthquake, it is hypothesized that the dynamic behavior of a moment-resisting frame can be studied by confining the inelastic behavior to the connections. The Alternative Dynamic Test method expounds on this hypothesis by using controllable actuators at the connection joints to replicate the inelastic behavior, reproducing the dynamic behavior of a steel moment-resisting frame structure more accurately.

Using scale models to represent the dynamic behavior of steel frame structures has its own limitations when the test material passes into the inelastic

range (because then scaling laws no longer apply). Failing to adjust for this nonlinearity could cause the scale model to behave significantly differently from its prototype. Implementing the Alternative Dynamic Test requires a reasonable model of the inelastic dynamic behavior of steel connections in the small-scale models. The use of a controllable joint mitigates the possibility of the scale model misrepresenting the actual structure, and helps simulate degradation in real time without physically damaging the structure. For instance, active control is critical when a connection behaves inelastically, since inelastic behaviors such as crack propagation, local buckling, heat dissipation, and plasticity do not scale geometrically. For example, based on the π theorem, Quintiere shows that heat dissipation varies by $s^{5/2}$, where s is the geometric scale factor. Active control of the connections maintains appropriate scaling laws and the integrity of the experiment. By this principle, the test method can be expanded to other materials with appropriate scaling taken into account.

1.3 Active Control

The Alternative Dynamic Test uses negative feedback to achieve an active control mechanism. The load is applied dynamically to the model (unlike in PsD tests) and the moment is measured at the controllable joints. Using this feedback from the system, the necessary rotation of the joint can be calculated dynamically and the controllers adjust the rotation in real time. An analytical model can also

be used to achieve this control, modeling the connections and testing the rest of the structure dynamically, however using the model is not truly a negative feedback mechanism and there would be a significant time delay. The analytical model is useful for proof of concept before the additional feedback systems are integrated into the experiment.

1.4 Research Objective

The objective of this research project is to demonstrate the feasibility of the Alternative Dynamic Test method. This will be demonstrated through the methodology of the test: applying appropriate scaling laws to model the dynamic behavior of steel frame structures. Selecting appropriate motors to actively control the test specimen, the motors will be characterized to develop an effective control algorithm. Finally, the experimental setup will integrate the desktop shake table system (including the linear encoder and linear motor) with the active control negative feedback loop to demonstrate the viability of the test method.

1.5 Outline of Thesis

This thesis has been organized into five chapters beyond this introduction. Chapter 2 will describe the Alternative Dynamic Test methodology and the integration of scaling laws with an actively controlled test specimen. Chapter 3 discusses the characterization of the servo motors for actively controlling the

model frame. Chapter 4 outlines the experimental setup and procedure for performing the Alternative Dynamic Test. Chapter 5 will examine the results of the research performed and provide analysis and commentary. Finally, Chapter 6 presents the conclusions, impact, and future work of this research project.

Chapter 2: Alternative Dynamic Test

Methodology

2.1 Scale Modeling

2.1.1 Need for Scale Modeling in the Alternative Dynamic Test

The Alternative Dynamic Test method uses scale modeling to represent the dynamic behavior of steel frame structures based on the working hypothesis that the inelastic behavior of the frame can be confined to the connections. This hypothesis is based on data from the 1994 Northridge earthquake and subsequent seismic events where fractures were discovered at or near the beam-column connection regions. If a full-scale dynamic test can capture the inelastic behavior of these joints, an actively-controlled model structure should perform likewise if properly scaled.

Using appropriate scaling laws is crucial for scale models to be accurate. When a material passes into the inelastic range, the scaling laws of linear-elastic materials no longer apply and failing to account for the nonlinearity can cause the scale model's behavior to vary significantly from the prototype. Behaviors including local buckling, crack propagation, plasticity, and heat dissipation do not scale linearly. For instance, Quintiere demonstrates through the π theorem, that

heat dissipation varies exponentially by $s^{5/2}$, where s is the geometric scale factor. Actively controlling the connections based on the Northridge hypothesis isolates the inelastic behavior to the joints and maintains appropriate scaling laws in the experiment.

Active control is often impractical in infrastructure applications, however, because the power requirement is excessive for full-scale structures. The motor power necessary to actively control average buildings and structures would potentially exceed the cost-benefit of installing them. Moreover in the midst of actual seismic events, power may not be available to the system, and so the effectiveness of an active control system would be uncertain. On the other hand, in controlled laboratory experiments, power is consistently available so power loss during the modeled seismic event is not an issue. The large power requirement remains an issue in the laboratory environment, however, and must be reduced to a reasonable level through proper scaling.

DC electric motors are effective for actively controlled structural applications because they affect a high static torque and can achieve large torques and rotation rates with proper gears or leverage. Static torques are necessary because an actively controlled system must be able to sustain reactions not only adjust to changing conditions in real time. Scale modeling can be utilized effectively in this experiment to reduce the motor power needed to control a test

specimen. To demonstrate the usefulness of scale modeling for this application, a structural analysis of the simple frame in Figure 2 will be conducted, along with an analysis of the strength requirement for the frame under seismic loading, which will lead to further discussions of reducing the motor power requirement in the subsequent subsections.

2.1.2 Structural analysis of simple frame

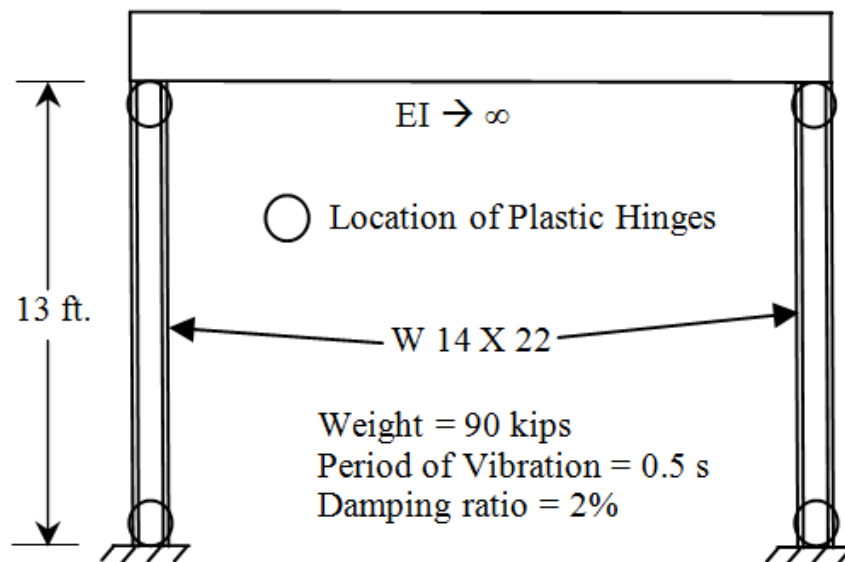


Figure 2 - Simple frame for analysis

The simple frame in Figure 2 consists of a rigid beam and two columns fixed to the base plane, which permits the columns to deflect in double curvature under load.

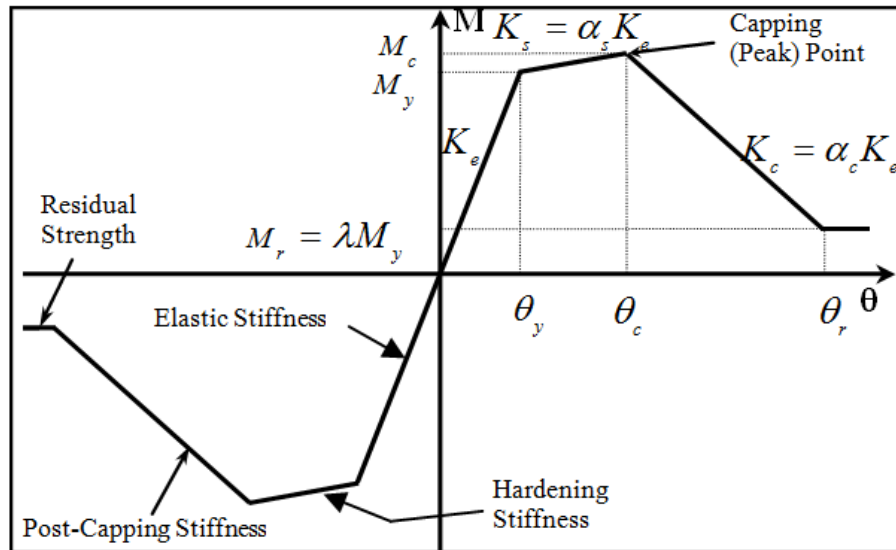


Figure 3 - Characteristic curve of moment-rotation relationship at plastic hinges

The plastic hinges in the simple frame depicted in Figure 2 are assumed to follow the characteristic curve in Figure 3. Following the analysis by Medina, the properties of the curve at the plastic hinges are:

- $M_p = 1660 \text{ k-in.}$,
- $K_e = 6EI/L = 221,962 \text{ k-in.}$,
- $\alpha_s = 0.03$,
- $\alpha_c = -0.06$,
- $\delta_c/\delta_y = \theta_c/\theta_y = 4.0$, and
- $\theta = 0$.
- Where M_p is the plastic moment capacity of the cross-section and θ is the rotation.

2.1.3 Strength demand under earthquake load

To estimate the moment-rotation response of the plastic hinges under seismic loading, the ground motion of the 6.7 magnitude 1994 Northridge earthquake is utilized. The horizontal component is taken from the Canoga Park Station record of the earthquake, NR94cnp, measured 15.8 km from the fault zone in stiff soil. Figure 4 depicts the 2% and 5% damped pseudo-acceleration response spectra for the NR94cnp record.

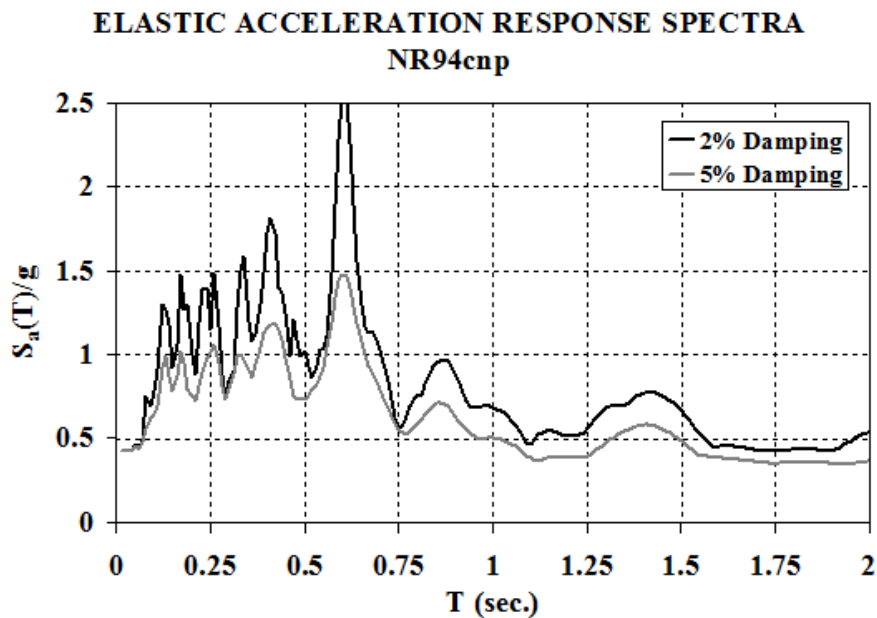


Figure 4 - 2% and 5% damped pseudo-acceleration response spectra for NR94cnp

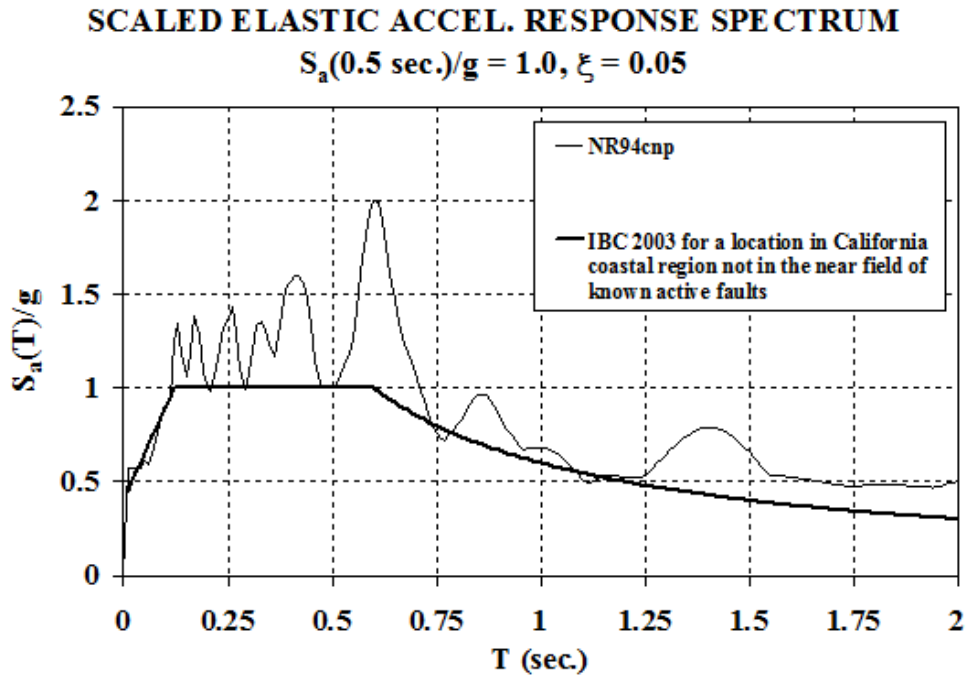


Figure 5 - Scaled ground motion spectrum for NR94cnp record

To determine if the record is consistent with the ground motion necessary for experimental evaluation, the 5% damped elastic acceleration spectrum in Figure 4 is scaled to $S_a(0.5 \text{ sec.}) = 1.0g$. The scaled ground motion spectrum for the NR94cnp record is shown in Figure 5, and the scaled NR94cnp record is found to be consistent with the IBC 2003 requirements for the appropriate region in California.

Having determined the record is acceptable, the scaled spectrum in Figure 5 is used to calculate the moment-rotation relationship of typical column ends [as

in (Medina 2007)]. The maximum required power is determined to be approximately 25 kW.

2.1.4 Using scale modeling to reduce motor power requirement

Using the maximum required power determined in the previous section with the Buckingham π Theorem as scaling law, the power needed to actuate a scaled model is found to be $25 \cdot S$ kW, where S is the model scale factor. For a 1/10 scale model, the power necessary for the motor would be approximately 2.5 kW. Nevertheless, a 2.5 kW motor is still quite powerful for experimental active control of a simple frame; with additional scaling, the power requirement can be reduced further.

Following our assumption that inelastic behavior in this experiment is confined to the joints, the remainder of the scale model structure can be assumed to have linear elastic behavior. With linear elastic behavior, scaling is linear with regards to stress and strain and displacement in the scale model, using a scale factor S as before. The geometric properties such as modulus of elasticity E can also be scaled linearly for the linear elastic members in the scale model. This allows us to scale the material properties as well as the dimensions of the model. Using members with a lower modulus of elasticity scales the required moment in each connection. For instance, assuming a steel prototype with $E=200$ GPa being scaled to an aluminum scale model with $E=70$ GPa, the scale factor for the

connection is 0.35, meaning the connection in the scale model will take a little more than a third of the moment that the original member would have to effect the same rotation. We will take advantage of this scaling property for the Alternative Dynamic Test because scaling the required moments in the connections will likewise scale the required motor power.

Table 1 - Comparison of motor requirements for various member materials

Member material	E (<i>GPa</i>)	Torque (<i>N – m</i>)	Power (<i>kW</i>)	Req'd speed (<i>RPM</i>)
Steel	200	640	2.5	3600
Aluminum	70	210	0.85	3600
Polymers	2 – 4	6– 10	0.050	3600

Table 1 demonstrates the effectiveness of scaling materials as well as dimensions for reducing motor power requirements. Using a softer metal such as aluminum over steel for the experimental model reduces the necessary forces and motor power requirement to almost a third of their original values. Furthermore, using various polymers can reduce the power requirement to as little as 50 W.

For this experiment a 1/10 scale aluminum frame will be used, with a motor power requirement of 85 W. (This calculation is shown in Chapter 3).

2.2 Active Control

To implement active control in the Alternative Dynamic Test procedure, an effective control algorithm must be developed to manage the servo motor actuators. Developing a control algorithm for an earthquake event is challenging because the loads and conditions are constantly changing and cannot be accurately known at every instant. As part of this research a negative feedback loop will be employed to establish active control.

A negative feedback loop uses data to close the gap between the current state and the desired state of an experiment. The dynamic responses of the test frame specimen to seismic loading will be measured through a sensor and “fed back” into the control system. The control algorithm will determine the variance between the actual and desired response. Based on the variance, the algorithm will calculate an appropriate response and apply it through the servo motors. The effectiveness of the response will again be measured and this process repeated to iteratively reduce the variance until the system is under control.

In the context of this experiment, using sensor data of the moment (torque) at the connection, the control algorithm will determine the appropriate rotation to correct the moment action. The control system will then apply a balancing torque through the desired rotation of the servo motor actuators.

The Alternative Dynamic Test is unique from PsD testing in this regard because it seeks to use concurrent dynamic test data from the test frame specimen to correct itself through real-time feedback. The PsD test utilizes an analytical model of the structure, rather than live structural data to calculate its response. This closed-loop negative feedback mechanism is advantageous for better characterization of the test specimen, but the control algorithm must account for the time delay in processing and actuating the commands.

The specific active control system developed in the experimental research for this project will be discussed in Chapter 4.

2.3 Error Approximation

An ancillary benefit of the active controlled Alternative Dynamic Test is a method for validating the experimental result through error approximation. As in all laboratory experiments and research, it is important to understand and subliminate known experimental errors. In the case of the Alternative Dynamic Test, there is a time delay present in the active control feedback loop while the servo motor is actuating the desired rotation. The use of a scale model magnifies this delay, increasing the frequency content by a factor of \sqrt{S} . Accounting for this tracking error is necessary to understand how closely the test specimen replicates prototype behavior.

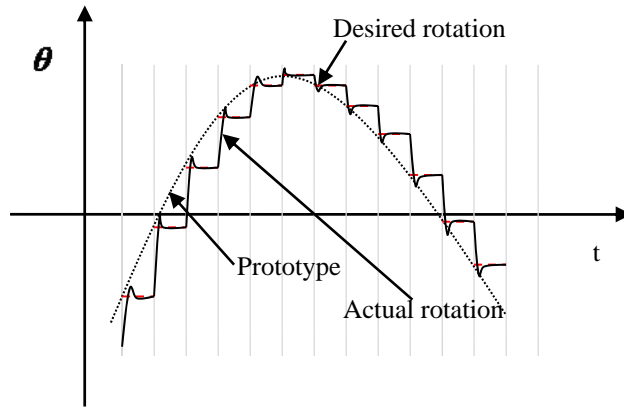


Figure 6 - Error in the implementation of the control algorithm

Figure 6 depicts the tracking error as the difference between the prototype curve and the actual rotation of the motor. Note the time lag in the actual rotation as opposed to the idealized prototype curve.

To approximate the tracking error (Medina 2007):

- Let θ_p be the rotation of the prototype connection given the measured moment (obtained from an analytical model)
- Let θ_d be the desired rotation that the controller attempts to match.
- Let θ_a be the actual rotation that the controller provides.

Where $\theta_p - \theta_a = 0$, the scale model perfectly mimics the prototype behavior. It is impossible to achieve perfect replication throughout the experiment, however, due to the time delay.

Let r be the ratio of energy $\left(\int_0^{T_d} M(\theta_p - \theta_a)dt\right) / \left(\int_0^{T_d} M(\theta_p)dt\right)$, where

- M is the moment measured at the connection, and
- T_d is the duration of the experiment.

If $|r| < \varepsilon$, then $|M_p \theta_p - M_a \theta_a| < \delta$, where

- $\varepsilon \ll 1$ is a sufficiently small number,
- M_p = moment of the prototype connection corresponding to the angle θ_p , and
- M_a = actual moment.

Using an analytical model of the connection, the difference in energy between the model and the controlled joint will produce a lower level bound of the error.

Chapter 3: Motor Characterization

3.1 Motor Requirements

The methodology discussed in section 2.1 will be utilized to determine the motor requirement for the experiment.

From section 2.1.3, the maximum required power of an un-scaled prototype is 25 kW. Considering the following parameters (per section 2.1.3):

- 1/10 scale model; scale factor $S = 0.1$
- Using aluminum instead of steel material; additional scaling of 0.35


The motor power requirement is determined to be $(25 \text{ kW})(.01)(.35) = .85 \text{ kW} = 85 \text{ W}$.

3.2 Motor Specification

Based on the experimental motor power requirement determined in section 3.1, the SpringRC SM-S4209M digital servo motor was selected for this research.

As shown in Table 2, the SM-S4209M provides 8.7 kg-cm of torque operating at the 4.8 V mode. This equates to 85.4 N-m of torque. Therefore the servo motor can meet the motor power requirement with $85.4 \text{ W} > 85 \text{ W}$ required.

Table 2 - SM-S4209M servo motor specification

SM-S4209M														
 <p>Show large image</p>					No. : SM-S4209M									
					Size: 41.3x20.7x40mm / 1.63x0.81x1.57in									
					Weight: 2.19oz									
					Specifications: Digital coreless fast servo,all metal gears,double ball bearing.									
										Application: electrocar,gas car,boat				
Item No: 5423094														
Product brochure Digital coreless fast servo,metal gear,double ball bearing.														
Products packing <ul style="list-style-type: none"> ◊ Pcking with clamshell Packaging content: Servo×1PCS、 Servo arm×1 bag Packaging specifications: Size-162.5×76mm、 Net weight-62g、 Gross weight-88.3g ◊ General packing (PE bag) Packaging content: Packing with PE bag Packaging specifications: PE bag size-120×85×0.07mm、 Netweight-62g、 Gross weight-79.1 														
Products specification								Technical parameters						
Size (in)					Weight		Wire	4.8V			6V			Rotation angle
								Speed	Torque		Speed	Torque		
A	B	C	D	E	g	oz	cm	sec/60°	kg·cm	oz·in	sec/60°	kg·cm	oz·in	
1.63	0.81	1.57	1.98	0.39	62	2.19	30.0	0.13	8.7	121.03	0.11	9.6	133.55	±60°

The servo motor is able to rotate $\pm 60^\circ$ in .13 seconds or 360° in .78 seconds. This allows the motor to actuate through up to 1.28 rotations/second at a torque of 8.7 kg·cm. These specifications are important because the Alternative Dynamic Test system requires rapid, real-time responses to the seismic stimuli, which the SM-S4209M delivers.

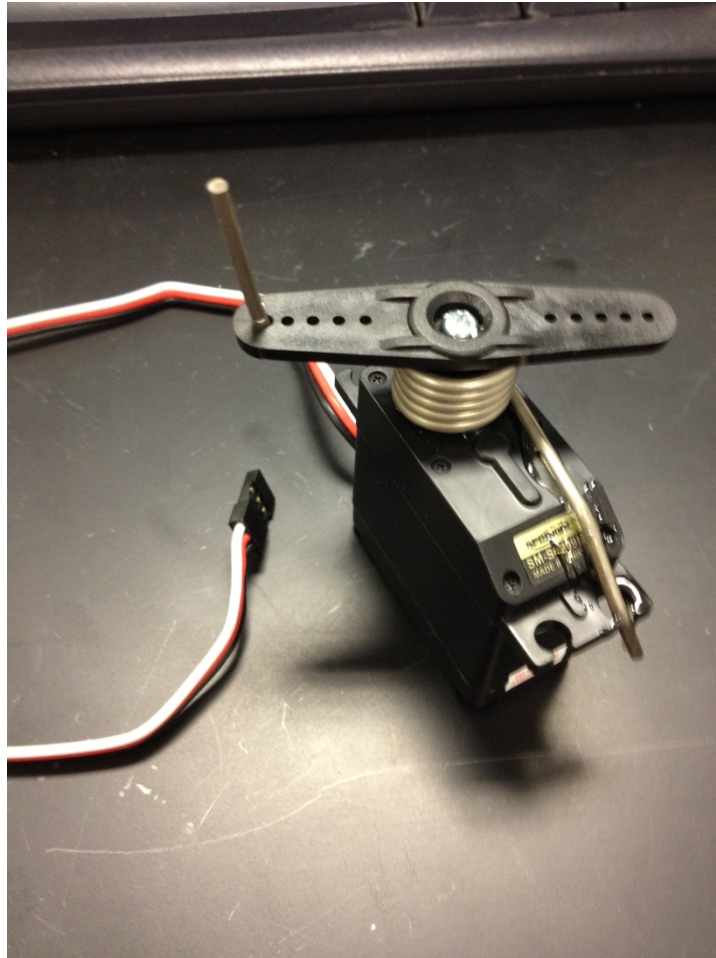


Figure 7 - Servo motor and spring assembly

For mounting the servo motors to the test specimen frame, each motor is integrated with a spring to provide stiffness at the joint connection.. The spring develops a linear moment-rotation curve and the motor can be used to fit the behavior of the frame to a non-linear moment rotation curve. This control of the connections maintains the linear elastic behavior of the structure.

3.3 Procedure

This procedure was followed to characterize the SM-S4209M servo motor and validate that an Arduino microcontroller can effectively actuate an active control system in this research experiment.



Figure 8 – Equipment setup for servo motor characterization

The Arduino microcontroller is connected to a laptop running Arduino 1.0 software to write, compile, and upload programs to the microcontroller via USB. The white lead wire from the Arduino microcontroller connecting to the breadboard is the control signal for the servo motor.

A power supply is needed to power the servo motor because when the motor is connected directly to the Arduino circuit board for power it draws too much current, which causes erratic movement of the servo motor and can potentially damage the Arduino microcontroller.

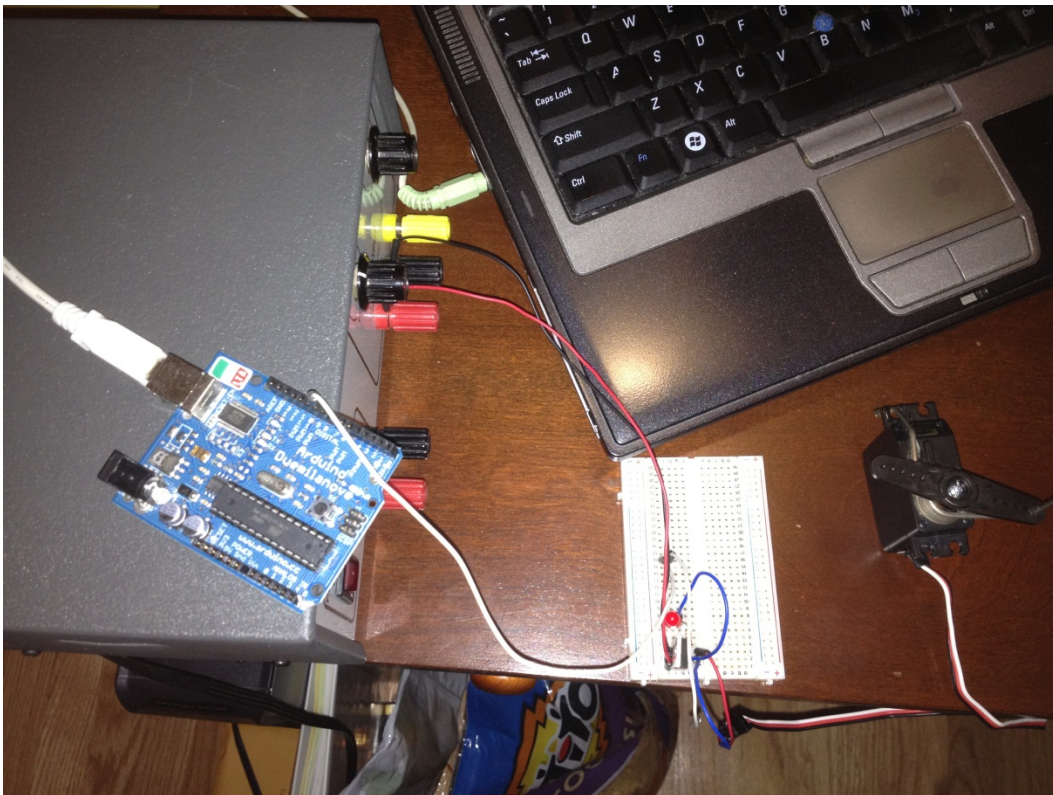


Figure 9 - Top down view of characterization circuitry configuration

The variable power supply provides voltage ranging from +1.5 to 15 V DC at 1 Amp of current. The voltage regulator on the breadboard modulates the voltage to a constant 5 V DC to power the servo motor at its 4.8 V configuration.

The breadboard in the figure below is setup to safely power the servo motor using the Arduino and an external power supply. The LED is wired in parallel to verify that the voltage regulator is working correctly and the servo motor is receiving power (in the figure, the LED is off, indicating the motor is not powered).

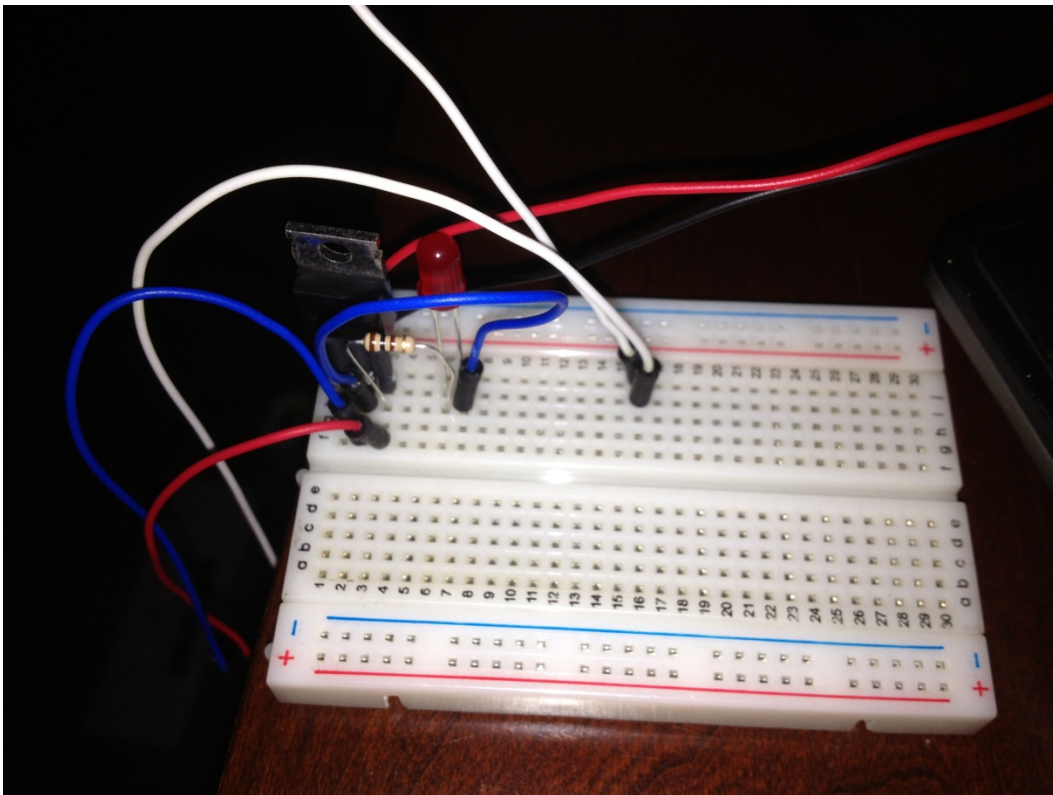


Figure 10 - Breadboard configured for servo motor characterization

The white leads provide control from the Arduino, which is simply patched through the breadboard. The red leads are positive power, while all the black and blue wires lead to the common ground pin at the center of the voltage regulator.

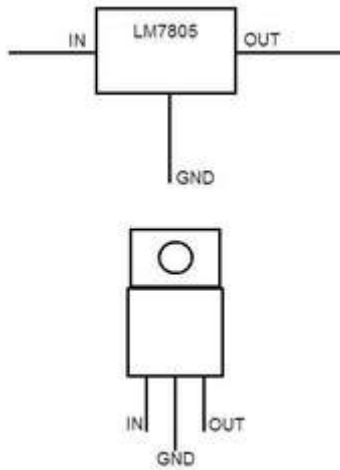


Figure 11 - Circuit diagram of voltage regulator

With control of the servo motor established using the code in Table 3, the servo motor is able to be directly controlled and the specifications evaluated.

Table 3 - Arduino code for controlling servo motor

```
#include <Servo.h>

Servo myservo;      // create servo object to control a servo
int pos = 0;        // variable to store the servo position

void setup()
{
  myservo.attach(9); // attaches the servo on pin 9 to the servo object
}

void loop()
{
  for(pos = 0; pos < 5; pos += .1) // goes from 0 degrees to 5 degrees
  { // in steps of .1 degree
    myservo.write(pos); // tell servo to go to position in variable 'pos'
    delay(2000); // waits 2s for the servo to reach the position
  }
  for(pos = 5; pos >= 1; pos -= .1) // goes from 5 degrees to 0 degrees
  {
    myservo.write(pos); // tell servo to go to position in variable 'pos'
    delay(2000); // waits 2s for the servo to reach the position
  }
}
```

Evaluation of the servo motor and spring assembly with an Arduino microcontroller demonstrated that it is capable of actuating the necessary control responses in experimental tests. Furthermore an Arduino microcontroller will provide adequate control of the system.

With the feasibility of the servo motor and control system validated, Chapter 4 outlines the full experimental setup for the Alternative Dynamic Test.

Chapter 4: Experimental Setup

4.1 Overview of Components

The Alternative Dynamic Test requires an integrated experimental setup of components which communicate and work together through data feedback to achieve active control of the test specimen.

A Kollmorgen linear motor acts as the primary actuator for the system, functioning as a desktop shake table to simulate earthquake events. To control the linear motor and establish the “absolute” position of the system, a Newall linear encoder is employed. The Newall encoder is mounted to the linear motor and a rod containing magnetic spheres which establish the position. This system functions independently to simulate the experimental seismic activity.

A parallel system controls the test specimen and tracks its position. An array of 6 NaturalPoint OptiTrack cameras follow tracking spheres mounted on the test frame to measure its relative position. This relative position can be compared to the absolute position of the encoder. The OptiTrack Tracking Tools software system also establishes its own “absolute” position based on the initial position of the specimen before the linear motor activates. As the seismic event is simulated, the camera tracking system will stream position data points through the NaturalPoint software into MATLAB where it is dynamically processed in real

time using the MATLAB Simulink package. These data can then be analyzed to compute the desired rotation of the controller motors.

Using an Arduino microcontroller and a supplementary power supply, the frame can be incrementally adjusted using servo motors mounted in the connection joints. This active control adjustment can be done dynamically, constantly adjusting based on the feedback loop of camera position data streaming from Natural Point Tracking Tools into MATLAB and then actuated through the Arduino.

The following sections will describe the function of each component in detail and how each integrates with the system to support the active control mechanism:

- Section 4.2 discusses the linear motor,
- Section 4.3 discusses the linear encoder,
- Section 4.4 discusses the camera tracking system,
- Section 4.5 discusses the data processing system, and
- Section 4.6 discusses active control using the Arduino microcontroller.

4.2 Linear Motor

The Kollmorgen direct drive linear motor is effectively used as a desktop shake table. It is the primary actuator in the experiment because the validation of earthquake engineered structures requires the experimental replication of earthquake events. The linear motor is capable of being accurately controlled (direct drive) to travel at the frequencies of a typical seismic event with linear accelerations exceeding 1 m/s.



Figure 12 - Kollmorgen Platinum DDL (Direct Drive Linear) motor

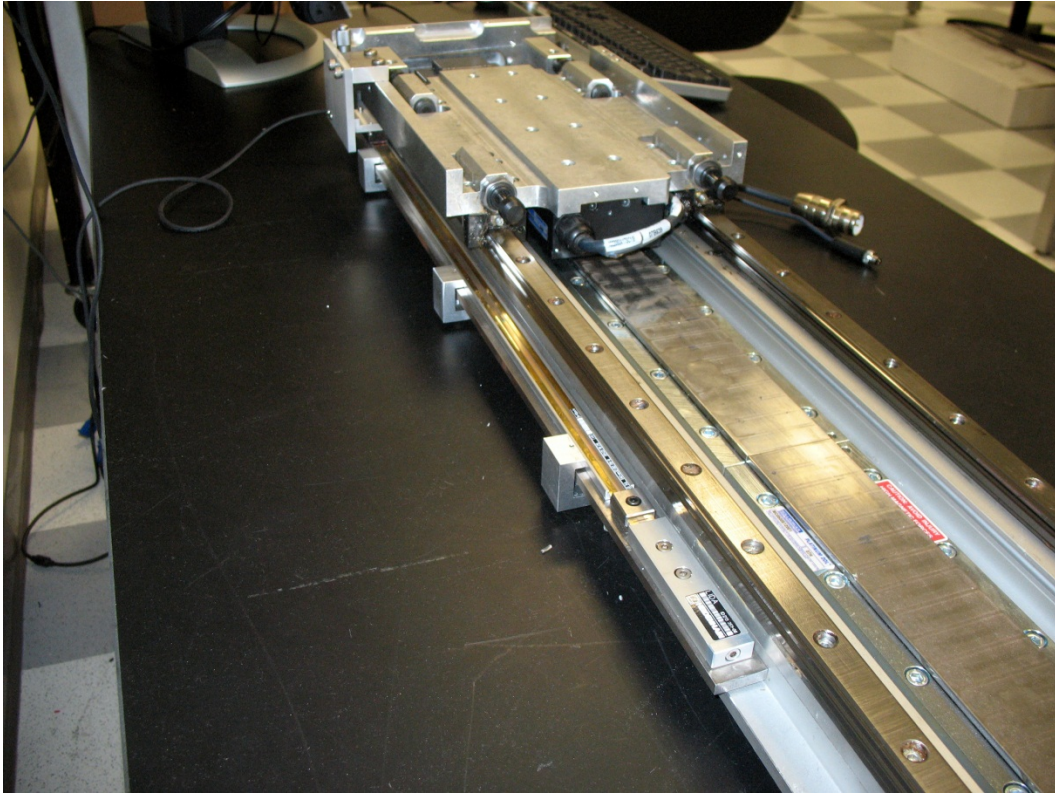


Figure 13 - Kollmorgen Platinum DDL (Direct Drive Linear) motor

4.3 Linear Encoder

While the linear motor is the critical actuator in this experiment, the linear encoder is the requisite sensor for controlling the actions of the motor. The high accelerations of the linear motor were a deciding factor in selecting linear encoders. The ability for encoders to read position data at high accelerations (exceeding 1 m/s in this case) can lead to a tradeoff between accuracy and maximum acceleration. In this case, some accuracy can be sacrificed because even in a 1/10 scale model of a building structure, knowing position to the nearest micron is not necessary. Fortunately, the encoders available for this research did not require that tradeoff and are able to provide surprising accuracy data at high speeds (up to 10 m/s).

Initially a Heidenhain LIDA series glass tape linear encoder was used to track the absolute position of the linear motor. It was discovered, however, that an exposed encoder would not function well in this laboratory setup due to environmental contaminants (e.g. lubrication grease from the motor being sprayed onto the encoder tape). It was decided to pursue a new encoder, which ultimately cost less to purchase new than repairing/replacing the Heidenhain system.

Searching for a replacement encoder system, the Newall SGH-TT was discovered. Like the Heidenhain LIDA encoder it utilizes a TTL differential quadrature signal, therefore it is compatible with the control box and cable

previously used for the Heidenhain encoder. The Newall SGH-series encoders operate on the principle of electromagnetic induction rather than glass optics. A drive coil within the reader head induces a sinusoidal current which emits an electromagnetic field. The magnetic field interacts with the ball bearings inside the steel rod to determine the position of the reader head as it traverses the scale.

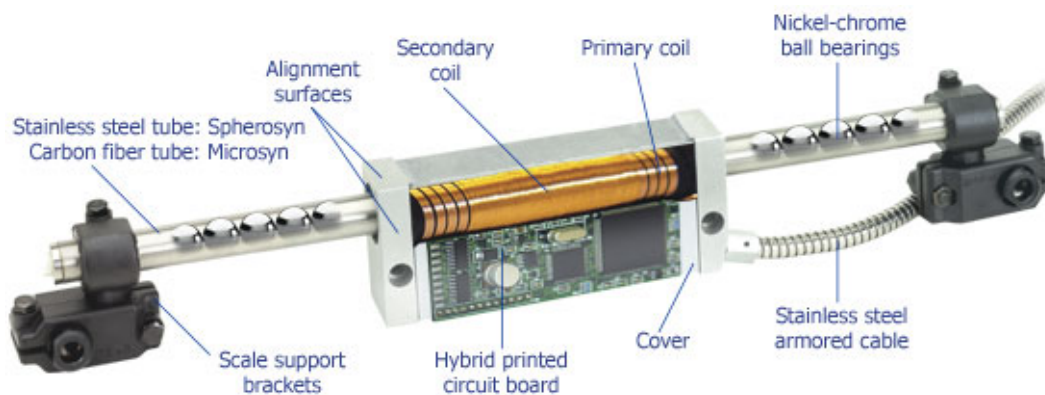


Figure 14 - Interior circuitry and layout of Newall SGH-TT encoder

One concern arose with using an electromagnetic inductive encoder: there was concern of electromagnetic interference because the linear motor uses very strong magnets to drive itself and it is necessary for the encoder to be mounted directly on the linear motor. Fortunately, due to the properties of magnetic fields, the magnetic force dissipates at a rate inversely proportional to the distance squared, so no interference will occur. The manufacturer suggested at least 0.5" separation between systems to preclude interference and this equipment setup has separation in excess of 2" from the two magnetic systems. Furthermore, the

Newall SHG-TT linear encoder is rated for harsher lab environments than ours; it is typically installed in machine shops and CNC machines.



Figure 15 - Newall SHG-TT Linear Encoder reader head

Mounting the linear encoder reader head required a custom mounting plate to be fabricated to secure the reader head to the linear motor assembly without eccentricity.

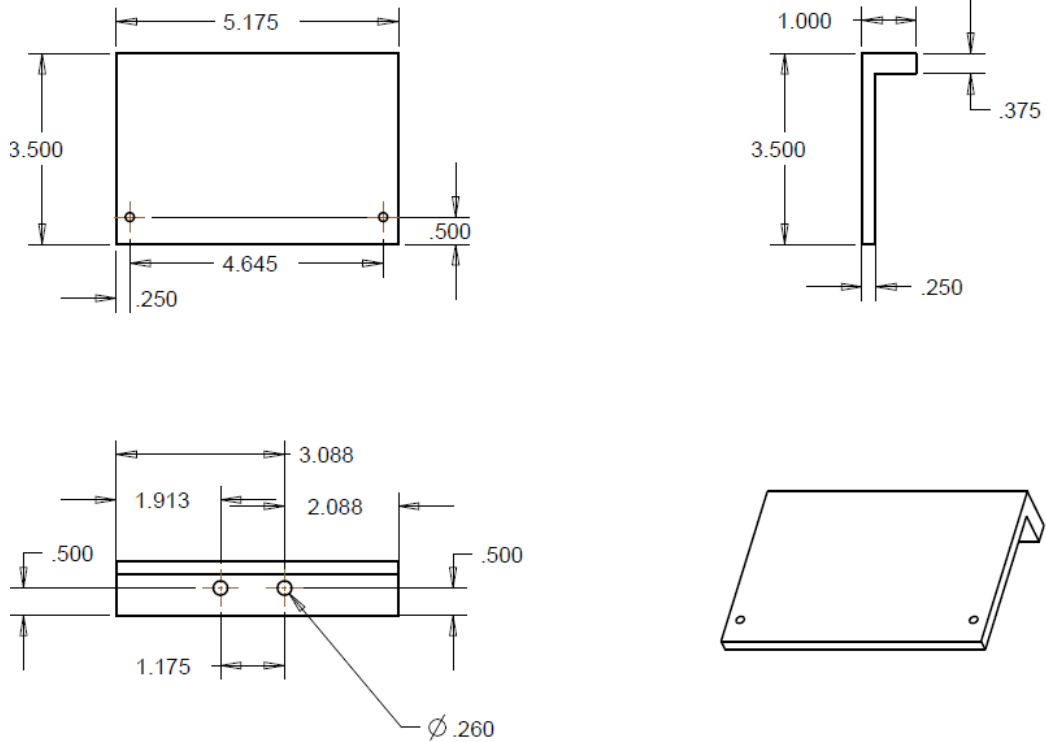


Figure 16 - Custom mounting plate for encoder reader head

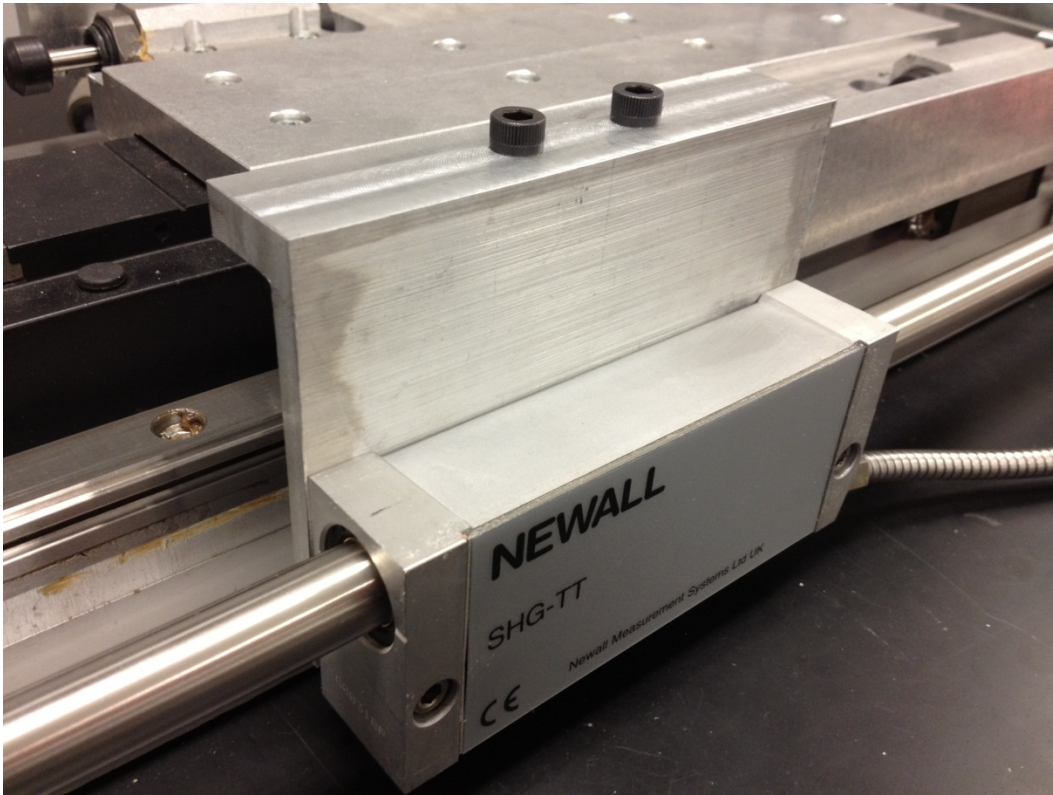


Figure 17 - Newall encoder mounted via mounting plate

Likewise, two custom anchor blocks were designed and installed for mounting the linear encoder supports securely to the base of the linear motor.

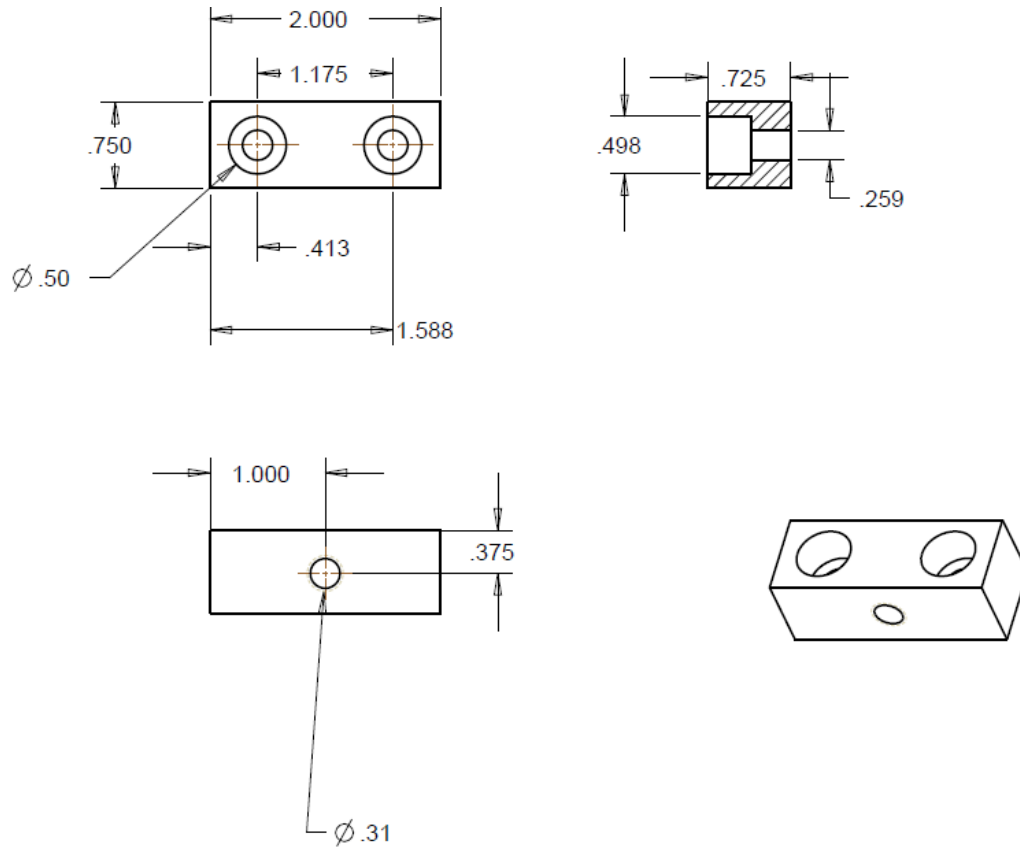


Figure 18 - Custom anchor block for linear encoder supports

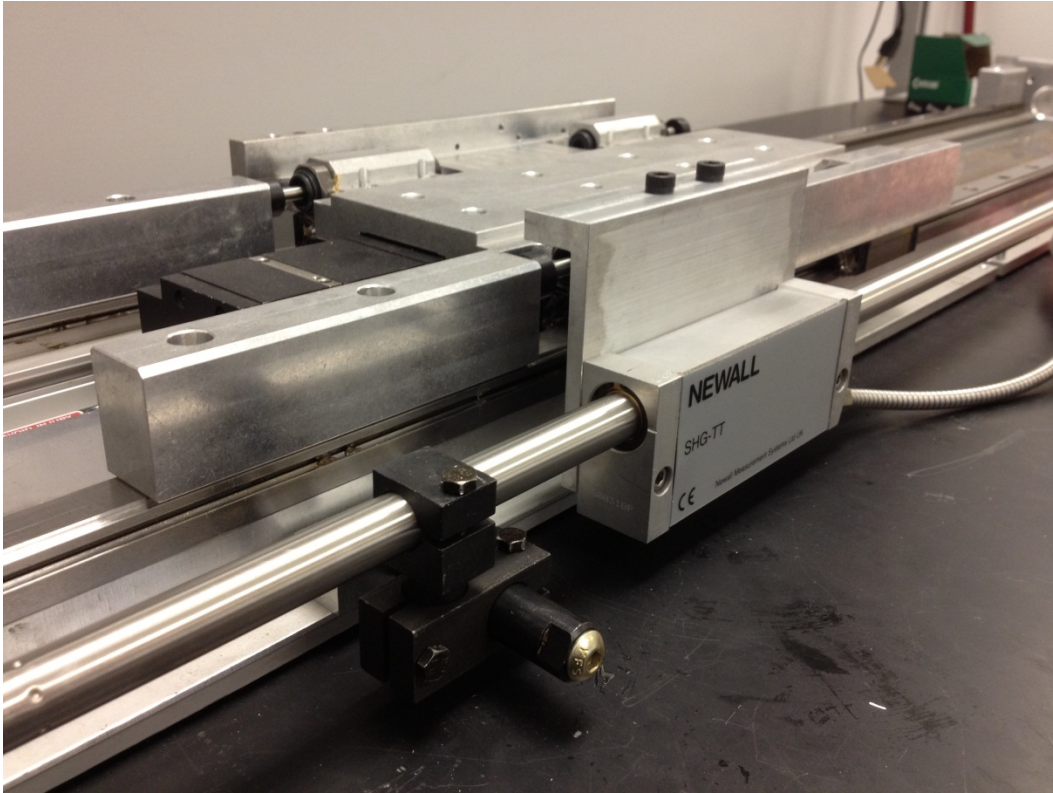


Figure 19 - Linear encoder mounted to linear motor

Note: The black linear encoder supports, seen in the foreground, secure the linear encoder to the base of the linear motor.

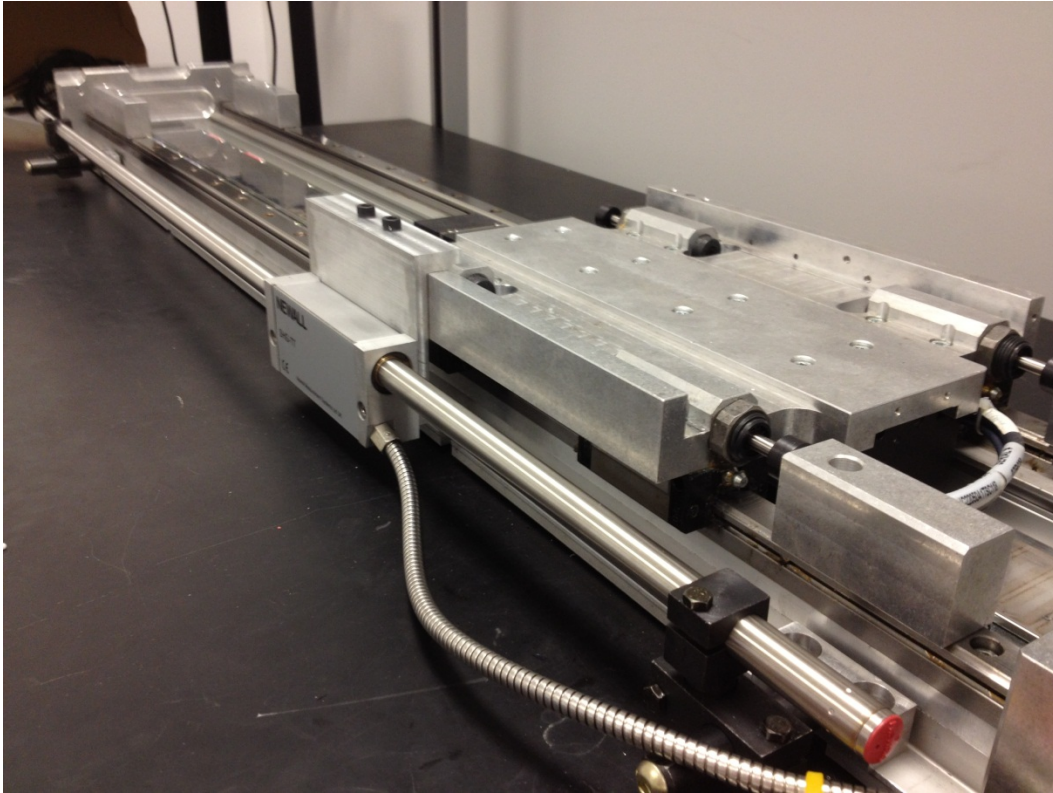


Figure 20 - Desktop shake table

Note: The custom anchor block depicted in Figure 18 can be seen in the foreground connecting the black linear encoder supports to the base of the linear motor.

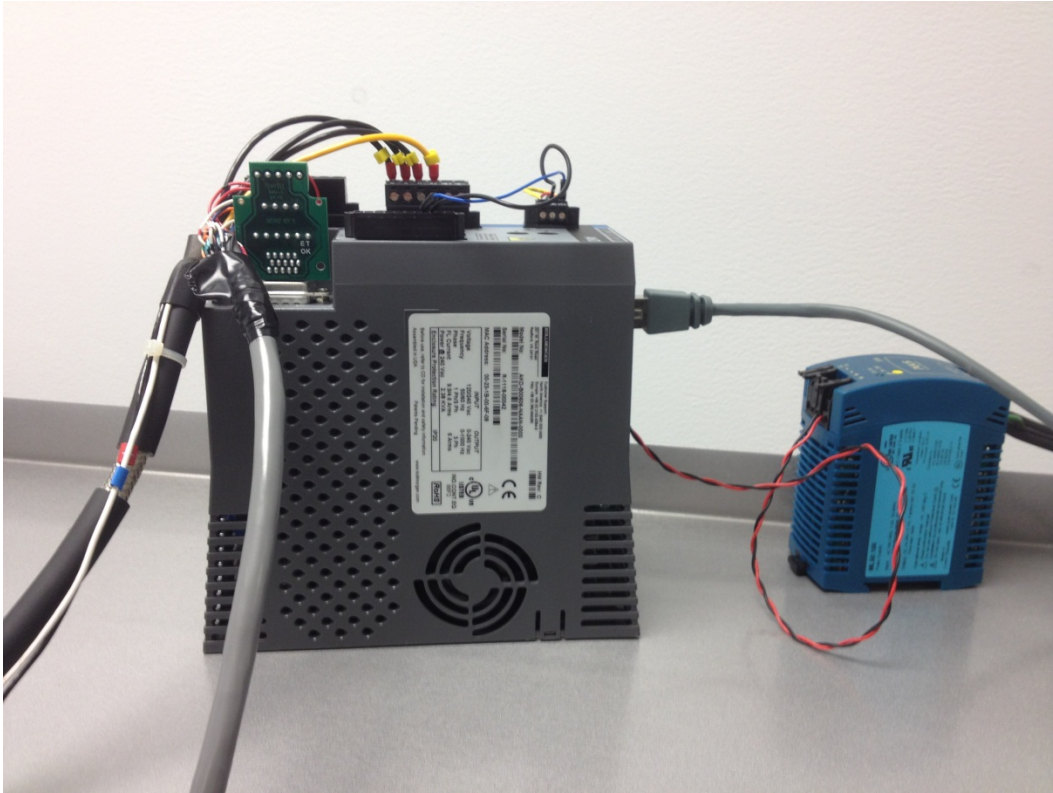


Figure 21 - Kollmorgen control box

The Kollmorgen control box in Figure 21 facilitates communication and control within the desktop shake table feedback loop. The gray lead on the left provides a reading of the linear encoder data and the black lead controls the linear motor. The gray Ethernet cable to the right facilitates communication with a computer interface running Kollmorgen Workbench software to analyze encoder data to accurately control the motor. This setup is depicted in Figure 23.

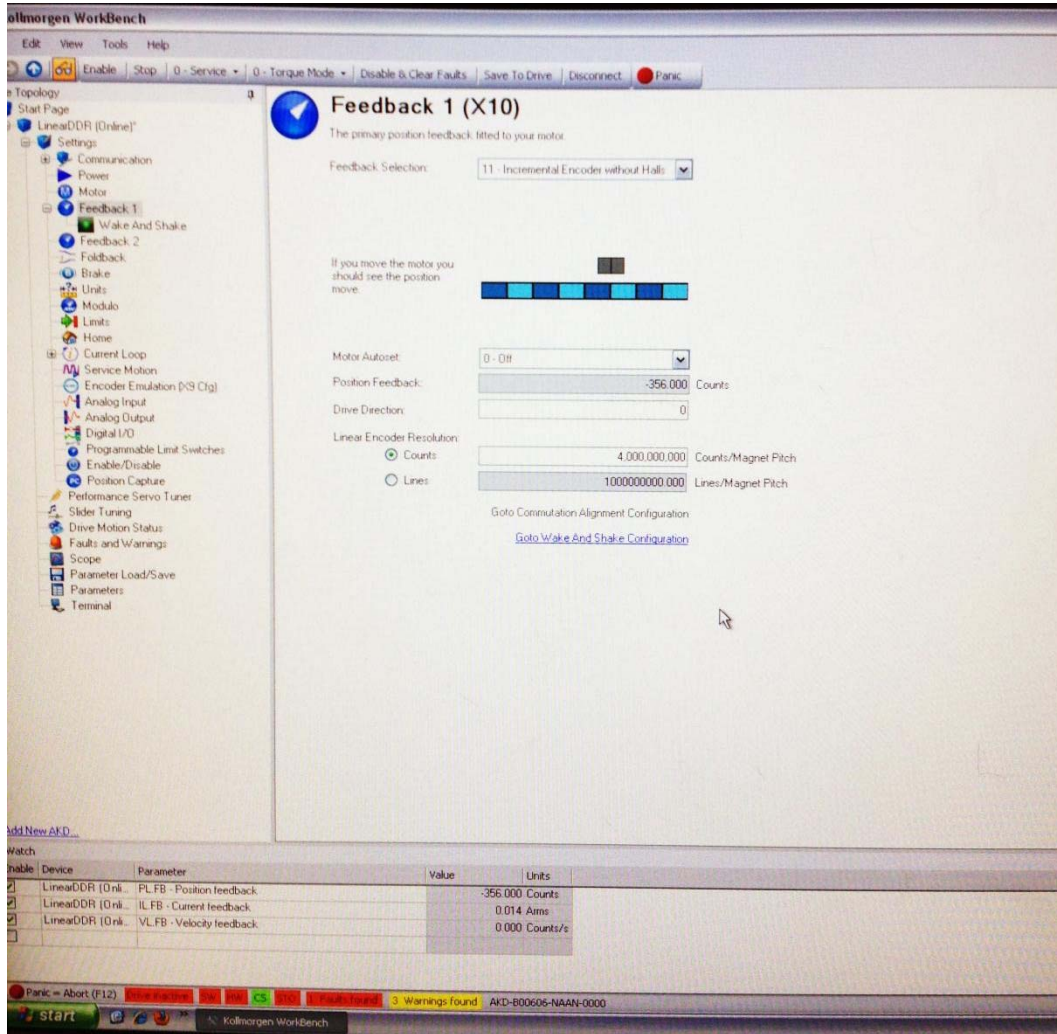


Figure 22 - Screenshot of Kollmorgen Workbench software

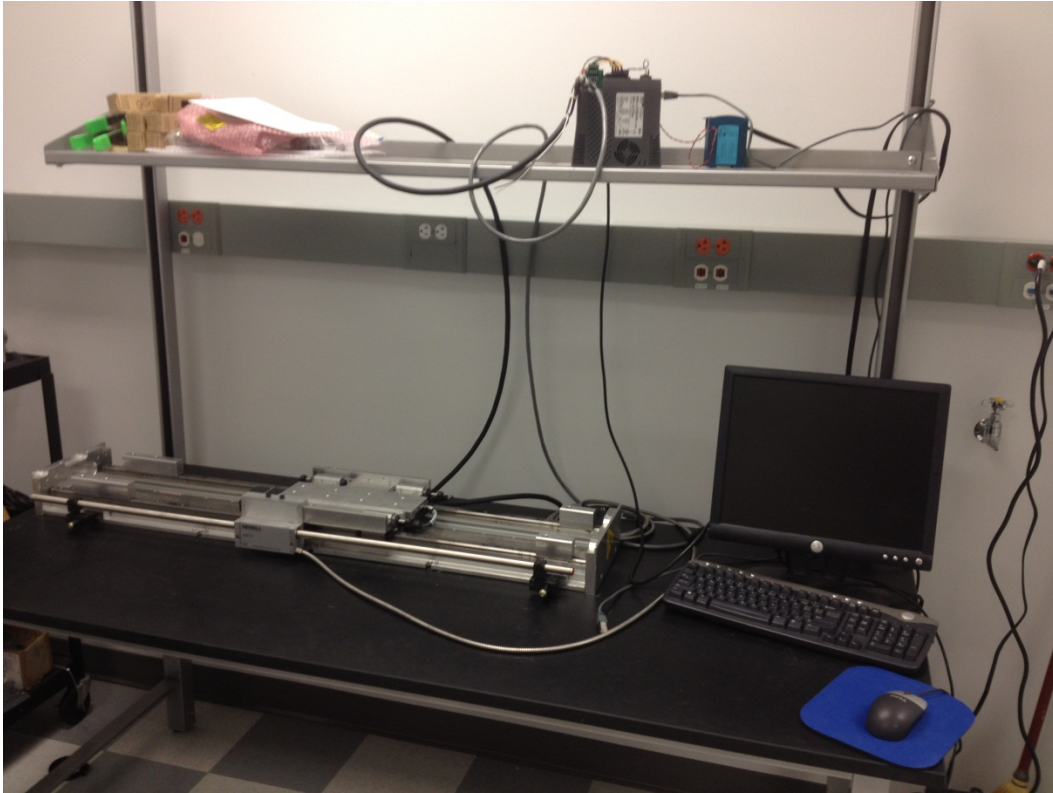


Figure 23 - Desktop shake table assembly

The desktop shake table assembly functions as an independent feedback loop controlling the experimental simulation of seismic activity. To control the test specimen itself, a parallel system of sensors independently provides data for controllers to manipulate and actively control the behavior of the specimen as explained in the forthcoming sections.

4.4 Tracking Cameras

An array of 6 high-speed optical cameras is used to track the test specimen. The NaturalPoint OptiTrack cameras are capable of accurately tracking the position of objects, even at the high accelerations of the linear motor.



Figure 24 - NaturalPoint OptiTrack camera

Using NaturalPoint's OptiTrack Tracking Tools software system, the camera array is first calibrated with a standard calibration wand to establish accurate 3-dimensional tracking. Next a ground plane is "set" in the dimensions of the linear motor. Feasibly this relative position could be compared to the

absolute position of the encoder, but for experimental purposes the position established by the Tracking Tools software is sufficient.

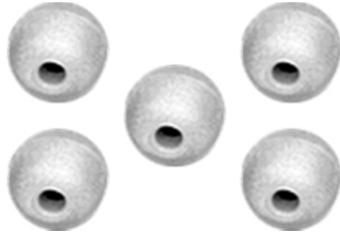


Figure 25 - NaturalPoint OptiTrack reflective markers (tracking spheres)

Optical tracking spheres are mounted to the test frame to measure its relative position as the linear motor simulates an earthquake event and the test specimen frame deflects, as depicted in Figures 26 and 27.

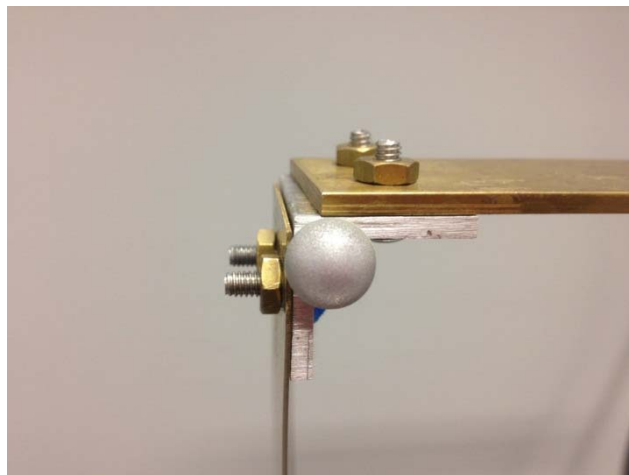


Figure 26 - Tracking sphere mounted in frame joint

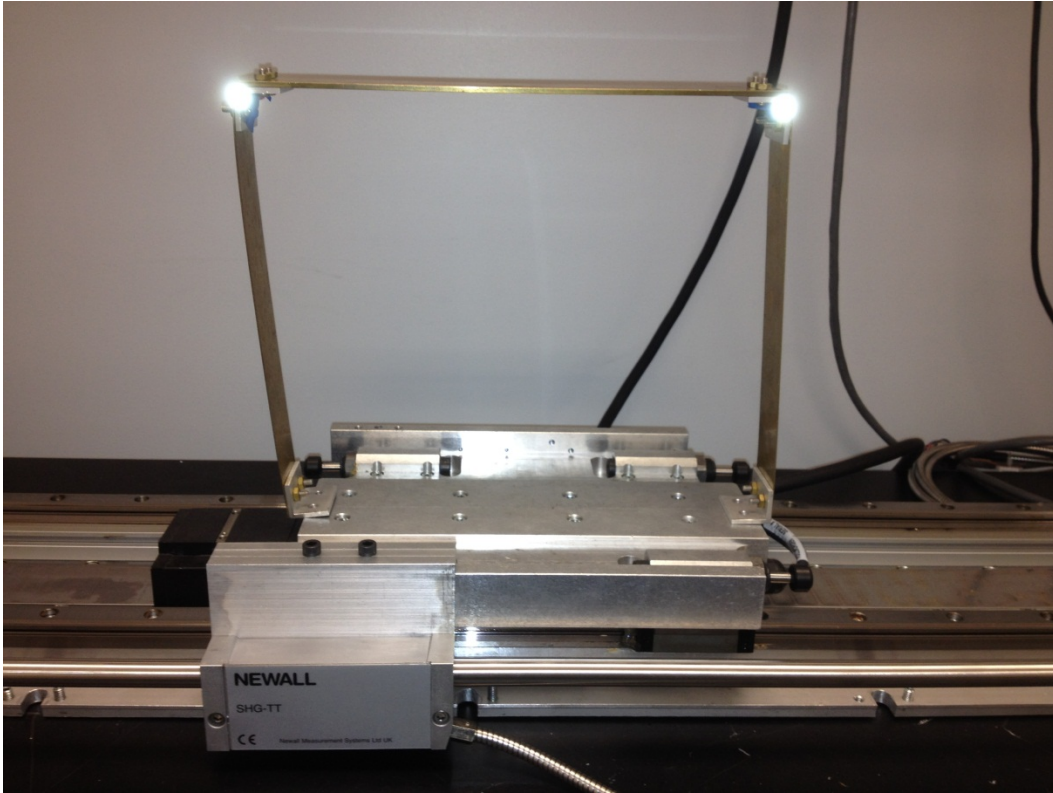


Figure 27 - Tracking spheres mounted to test frame



Figure 28 - Experimental array of NaturalPoint OptiTrack cameras

Note in Figure 28 above that the cameras are mounted at different heights and distances to provide better 3-dimensional tracking. This camera arrangement, as opposed to a straight line, results in better calibration and a higher correlation factor of the final position.

4.5 Processing

As the experiment progresses, the NaturalPoint OptiTrack Tracking Tools camera software streams the position data into MATLAB using the TT_Tools_demo m-file in Table 4. MATLAB & Simulink process the data points and compute the necessary rotation for the controller motors.

Table 4 - TT_Tools_demo m-file

TT_Tools_demo(project_file)

```
function TT_Tools_demo(project_file)
% TT_Tools_demo(project_file)
%
% This function demonstrates basic functionality of the Tracking Tools API
% from Natural Point (to be used with Optitrack). Before use it is
% essential to have calibrated cameras and created the desirable
% trackable/s and save these in a project file. The project file is then
% passed to the function and the library loaded if need be before
% attempting to plot any data
%
% Input - project_file - a string containing path and filename for the
%           project file that is to be used (default value assigned if
%           not assigned)
%
% Written by Glen Lichtwark, University of Queensland, Australia
% Last updated: 22nd Jan 2010
% Please acknowledge in any academic papers which may utilise this code

if nargin < 1
    project_file = 'C:\WAGMAN\Test.ttp';
end

% load the NPTrackingTools library if it is not already loaded
if ~libisloaded('NPTrackingTools')

addpath('C:\WAGMAN\NaturalPoint\TrackingTools\lib'); % change if necessary
addpath('C:\WAGMAN\NaturalPoint\TrackingTools\inc'); % change if necessary

[notfound,warnings]=loadlibrary('NPTrackingTools','NPTrackingTools.h');
end
```

```

% libfunctionsview NPTrackingTools --> use this to see available functions

% initialise cameras
calllib('NPTrackingTools', 'TT_Initialize');

% load the project file which sets up cameras correctly
calllib('NPTrackingTools', 'TT_LoadProject', project_file);

%define the outputs types from TT_TrackableLocation function
X = 0;Y = 0;Z = 0;
qx = 0;qy = 0;qz = 0;qw = 0;
yaw = 0;pitch = 0;roll = 0;

figure(1)
clf
set(gcf,'Position',[127 73 933 602])

TC = calllib('NPTrackingTools', 'TT_TrackableCount');

TrackableNum = TC-1; % change this value to view different trackable object (starts at 0)

%loop through and plot the marker positions using frame results
for i = 1:500

    M = [];

    %update frame and get time stamp
    calllib('NPTrackingTools', 'TT_UpdateSingleFrame');
    D.T(i) = calllib('NPTrackingTools', 'TT_FrameTimeStamp');

    %find out how many markers are visible store data for X Y Z coordinates
    %of each
    marker_count = calllib('NPTrackingTools', 'TT_FrameMarkerCount');
    for j = 1:marker_count
        M(j,1) = calllib('NPTrackingTools', 'TT_FrameMarkerX',j-1);
        M(j,2) = calllib('NPTrackingTools', 'TT_FrameMarkerY',j-1);
        M(j,3) = calllib('NPTrackingTools', 'TT_FrameMarkerZ',j-1);
    end
    D.dat(i) = {M};

    % find the location of any trackable and plot the XYZ position on one
    % plot and euler angles on another

    [X,Y,Z,qx,qy,qz,qw,yaw,pitch,roll] = calllib('NPTrackingTools',
'TT_TrackableLocation',TrackableNum,X,Y,Z,qx,qy,qz,qw,yaw,pitch,roll);
    D.trans_dat(i,:) = [X Y Z];
    D.rot_dat(i,:) = [yaw pitch roll];
    % plot data --> note that this slows the frame rate considerably so
    % only do it every now and again

```

```

if rem(i,4) == 0
    subplot(2,2,2), plot(D.T-D.T(1), D.trans_dat)
    xlabel('Time (s)?')
    ylabel('Object Position (m)?')
    subplot(2,2,4), plot(D.T-D.T(1), D.rot_dat)
    xlabel('Time (s)?')
    ylabel('Object Orientation (deg)?')

    % make 3D plot of marker positions and the trackable position
    if ~isempty(M)
        subplot(1,2,1), plot3(M(:,1),M(:,2),M(:,3),'ko','X,Y,Z','ro');axis equal
        axis([-0.4 0.4 -0.4 0.4 -0.4 0.4])
        xlabel('X')
        ylabel('Y')
        zlabel('Z')
    end
    drawnow
end

end

calllib('NPTrackingTools', 'TT_Shutdown')

```

Note: the m-file code was altered (as recommended by the author) to indicate the file location of custom NaturalPoint libraries to be called and the Tracking Tools files (.ttp) for data streaming.

Without parallel processing, the laboratory computers are unable to simultaneously gather the data in the Tracking Tools software and stream it into MATLAB. Attempting to do both results in fatal errors in MATLAB and the Tracking Tools software freezing and crashing. Therefore two computers are necessary for data processing: one to acquire the position data and a second to stream it into MATLAB for analysis and computation.

Note in Figure 29 that the left computer runs the Tracking Tools software and gathers the data which is then accessed by the right computer and streamed into MATLAB. The right computer processes the data to inform the Arduino microcontroller how to control the servo motors for incremental adjustment of the test specimen frame.



Figure 29 - Data processing computers

4.6 Arduino Active Control

The active control feedback loop which governs the Alternative Dynamic Test specimen is depicted in Figure 30 below:

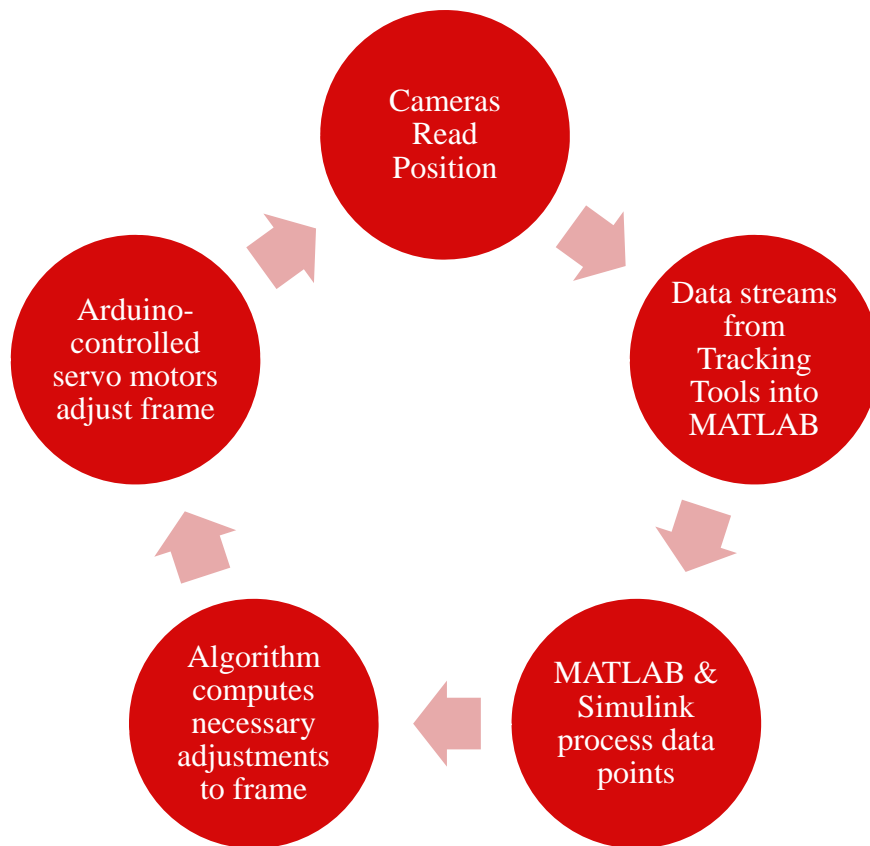


Figure 30 - Active Control Feedback Process

The final step in the feedback loop is the Arduino-controlled servo motors adjust the frame based on computations made by the data processing computer.

Using an algorithm to determine the exact rotation of the frame that is necessary, this adjustment is effected through the Arduino microcontroller.

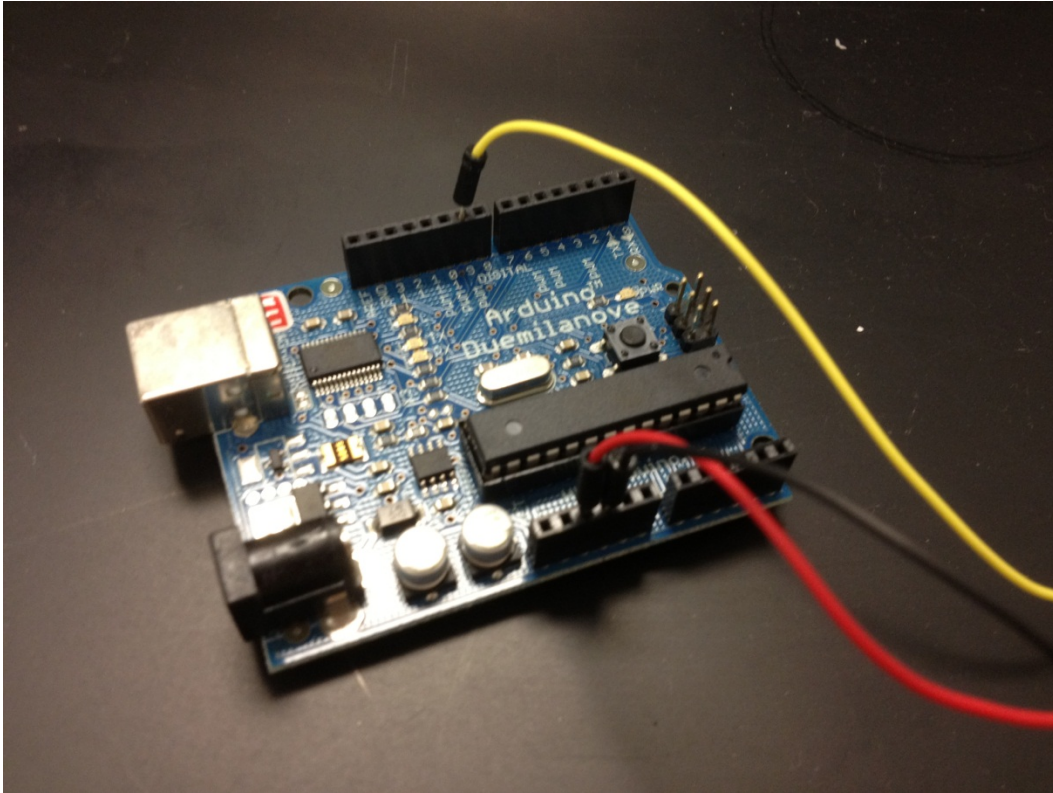


Figure 31 - Arduino Duemilanove Microcontroller

Chapter 5: Results and Analysis

5.1 Commentary

The crux of the research focus has been bringing the experimental setup online since my participation in this research began in September 2011. The Kollmorgen linear motor had been delivered to the BAE Systems Control Lab in 3209 Kim Engineering Building after the Heidenhain linear encoder was mounted to the motor base by the Electrical and Computer Engineering Technical Operations. The Heidenhain encoder is shown in Figure 32 mounted to the base of the linear motor.

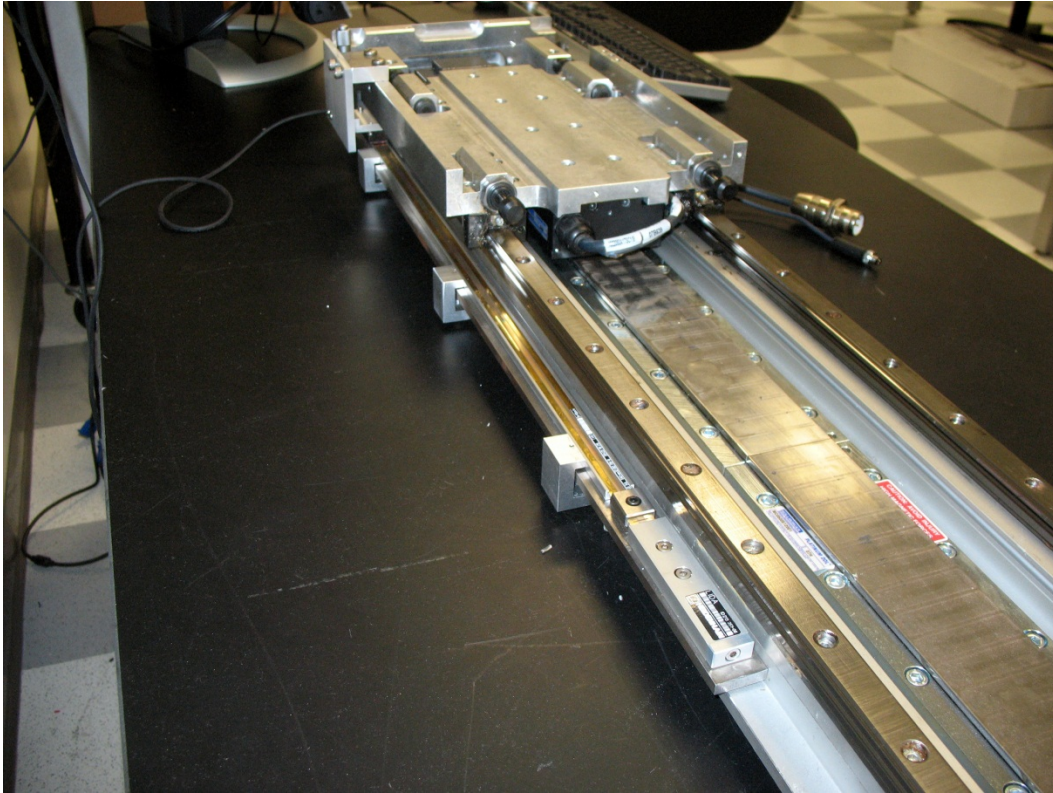


Figure 32 - Kollmorgen linear motor with Heidenhain encoder mounted

I was first tasked with bringing the desktop shake table assembly online and concurrently integrating the camera tracking system with the MATLAB interface. From that starting point, my research focus would then expand as milestones were achieved.

Mac Roberts of Eagle Engineering generously donated his time to help setup the linear motor because he has extensive experience with rotary motors but wanted to learn more about their linear counterpart. As his work brought him near College Park, Mac came by the lab and setup the Kollmorgen control box and

wired a cable to connect the linear encoder. The encoder was successfully interfaced with the control computer running Kollmorgen Workbench through an Ethernet connection. The encoder readings, however, were erratic and inconsistent; moving the encoder from a “zeroed” position to the other end of the scale and back did not return the readings to zero as expected. In fact, moving the encoder at all caused the readings to jump and continue moving even if the motor was still. Some sort of positive feedback in the system amplified the encoder counts and once it began the error continued propagating. Until the linear encoder was capable of providing accurate position data, the linear motor could not be controlled.

Mac and I attempted to troubleshoot the problem through the encoder manufacturer Heidenhain. It was unclear to their technicians whether the encoder was damaged or dirty (or both) and recommended evaluating the encoder head professionally and properly cleaning the tape. [Note: the Heidenhain linear encoder used glass optics to read its position as opposed to the magnetic encoder currently used from manufacturer Newall].

A regional specialist Jon Palmer from Endeavour Engineering (of Frederick, MD) was ultimately recommended by the Heidenhain technical support technicians to evaluate the encoder head onsite. Special Heidenhain evaluation equipment was ordered for the evaluation and Jon determined that the tape

(purchased used) was improperly installed. The tape was not uniformly adhered to its support structure, causing ridges and regions of unequal thickness to form in areas without adhesive bonds. These regions and ridges caused the linear encoder head to improperly read the markings on the tape, leading to the erratic data readings. It is also quite possible that the reader head itself is damaged, which would account for the positive amplification of the data errors experienced during troubleshooting. After Endeavour Engineering's evaluation in January, we moved to select and purchase a new encoder for the research project.

The Newall encoder was identified and purchased in February as a more robust alternative to replacing the Heidenhain encoder. Using magnetism to read the encoder position, the new Newall encoder would be more resilient in our laboratory environment and eliminate the potential for errors due to optical misreadings from the glass tape. The encoder was delivered in early March, and the ECE Technical Operations crew was brought in once again to design a plate and brackets for mounting the encoder head and support systems to the linear motor.

The mounting plate was originally slated for manufacture over spring break in mid-March, but material shortages and limited manpower delayed completion of the parts until early April. Despite these setbacks, the linear encoder was finally mounted and ready to be tested for accuracy.

Mac returned to the lab and found the encoder to be working accurately. He proceeded to wire the linear motor and work to power it into Wake and Shake mode through Kollmorgen Workbench for evaluation. Thankfully the linear motor is functional and we are working to determine the proper motor phasing to establish full control over its motion. Once the motor is configured properly it is seamlessly integrated with the position data from the linear encoder through the Kollmorgen software, establishing a complete feedback mechanism. At that point, the desktop shake table system will be fully operational.

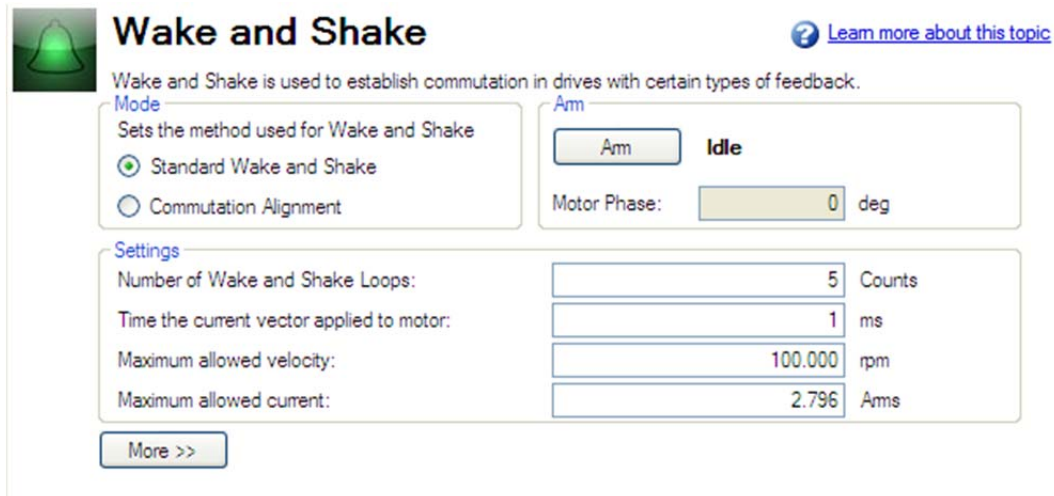


Figure 33 - Linear motor configured in Wake and Shake mode in Kollmorgen Workbench

Turning attention to the active control system, work continued concurrently to bring this system online with the desktop shake table. In the fall 2011 semester the motors and springs used in this research were identified and

ordered and methods for combining them discussed. Ultimately the assembly used in the research was decided on and constructed.

Likewise, attention was paid to the camera tracking system and re-establishing the Tracking Tools-MATLAB connection developed by previous researchers, but expanding it to two computers for pseudo-parallel processing. Since running MATLAB and NaturalPoint Tracking Tools simultaneously on the same computer causes both programs to freeze and crash, two networked computers were used for data processing instead. The hard drive of the slave computer running Tracking Tools was mapped to the master computer running MATLAB and Simulink so the streaming data file could be remotely accessed and analyzed.

Finally as setbacks in other systems precluded the opportunity for experimental evaluation of the fully integrated Alternative Dynamic Test system, additional attention was paid to characterize the servo motors. This successful characterization, considered with the status of other systems in the research project demonstrates the feasibility of the Alternative Dynamic Test. The desktop shake table system is only weeks away from being operational and fully integrated with the active control system of tracking cameras and servo motor actuators. But the primary objective of this research – proving the feasibility of the Alternative Dynamic Test – is achieved because each sub-system is

operational or nearly operational and expected to be fully functional in the very near future.

While the goal to go beyond the original research objectives is unachieved at the writing of this thesis, the trajectory of this research brings us extremely close to a successful proof of concept experimental test.

Chapter 6: Conclusions and Future Work

6.1 Conclusions

An experimental setup for the Alternative Dynamic Test was implemented with the goal of demonstrating the feasibility of the Alternative Dynamic Test method. The experimental setup utilized the methodologies of scale modeling and active control to represent the dynamic behavior of steel frame structures. Servo motors were characterized as actuators of the active control system, using a negative feedback loop to determine the appropriate moment rotational response to experimental seismic events. Based on these results, the following conclusions can be drawn:

- (1) The Alternative Dynamic Test method is a feasible alternative to conventional full-scale shake table tests and pseudo dynamic tests. Though the entire system is not fully functional, the desktop shake table system is very close as is the active control system. Each subsystem has a reasonable expectation of functioning, thereby assenting that the system itself achieves this primary research objective.
- (2) Employing appropriate scaling laws can achieve scale reductions in dimensions as well as material strength. With the inelastic behavior of the test specimen frames confined to the connections, the frame members can

be expected to exhibit linear elastic behavior, allowing for linear dimensional scaling. Comparing the moduli of elasticity of the original and substitute materials can also produce a linear scale factor that further scales the test specimen and reduces the power requirement for motors.

- (3) An actively controlled structural system can be effectively managed by using a negative feedback loop. Using data from the connections, the control algorithm determines an appropriate corrective moment rotation and actuates the desired rotation via the servo motors. As this process repeats, the principle of negative feedback is applied to iterate until to the desired level of control is achieved.
- (4) The Alternative Dynamic Test, with its ability to dynamically evaluate structural earthquake engineering designs through experimental validation, provides an opportunity for academic advancement of performance-based engineering design concepts in the earthquake engineering field.

6.2 Future Work

Through collaboration between the Department of Civil and Environmental Engineering, the Institute for Systems Research, and the Department of Electrical and Computer Engineering at the University of Maryland, College Park, the experimental setup used for this thesis is available to students for further research in structural earthquake engineering. The Alternative Dynamic Test system is located in the BAE Systems Control Lab in the Kim Engineering Building at University of Maryland and can be incorporated into the curricula and research activities of both departments.

In the immediate future, work continues in order to validate the Alternative Dynamic Test experimentally. The linear motor will be fully operational in the very near future, bringing the desktop shake table system online. To enable the shake table system to replicate seismic events for experiments, control using MATLAB software will be developed. This will allow for the use of complex motor commands and oscillation patterns like the NR94cnp spectrum from the 1994 Northridge earthquake. Moreover, MATLAB software is already available and being used in this experiment and in the BAE Systems Control Lab. On the other hand, to bring the active control system online, it is necessary to configure its parts to work together for active control and feedback. The camera system is integrated with MATLAB and Simulink for data

acquisition and processing, and further development of a control algorithm will allow the entire system to be contained within MATLAB, ultimately executing control through an Arduino microcontroller. With the implementation of MATLAB in each system, the Alternative Dynamic Test experimental setup will be fully operational and prepared for proof of concept experimentation.

As the University of Maryland develops additional research capabilities for structural engineering, this test setup will be an invaluable educational tool. The scale model with controllable joints can be used to demonstrate an earthquake's effect on structures; an educational user could create a joint with different behavior and observe how the changes in joint behavior affect the structure's performance on the shake table. This demonstration tool can be enlightening for pre-college students (for prospective student events and research open house events like Maryland Day), as well as for undergraduate and graduate students.

Furthermore, this project presents an excellent academic opportunity for further graduate-level degree research as a premiere example of structural engineering research at the University of Maryland. This research enterprise could be expanded to include support from undergraduate research assistants, and provide additional undergraduate research opportunities that are highly sought after. What is more, the presence of the research in the BAE Systems Controls

Lab in the A. James Clark School of Engineering's flagship Kim Engineering Building creates great opportunity for this project to be showcased among other prestigious labs.

Bibliography

- Aktan, H.M. (1986). "Pseudo-Dynamic Testing of Structures," *Journal of Engineering Mechanics*, 112(2): 183-197.
- Boresi, Arthur P., and Schmidt, Richard J. (2003). *Advanced Mechanics of Materials*. John Wiley & Sons, Inc., New Jersey.
- Chung, L.L., Reinhorn, A.M., and Soong, T.T. (1988). "Experiments on Active Control of Seismic Structures," *Journal of Engineering Mechanics*, 114(2), 241-257.
- Mazzoni, Silvia, et al. (2009). *Open system for Earthquake Engineering Simulation User Command-Language Manual*. Pacific Earthquake Engineering Research Center, University of California, Berkeley.
- Medina, R.A. and Krawinkler, H. (2005). "Strength Demand Issues Relevant for the Seismic Design of Moment-Resisting Frames," *Earthquake Spectra*, 21(2), 415-439.
- Medina, R.A. (2007). "Alternative Dynamic Testing by Active Control" National Science Foundation.
- Medina, R.A. (2004). "Story Shear Strength Patterns for the Performance-Based Seismic Design of Regular Frames," *ISET Journal of Earthquake Technology*, 41(1), 101-125.
- Mercado, M.W. (2011). A Hybrid Testing Platform For Realistic Characterization of Infrastructure Sensor Technology." *Digital Repository at the University of Maryland*. Retrieved from <http://hdl.handle.net/1903/11567>
- Nakashima, M., Kato, H., and Takaoka, E. (1992). "Development of real-time pseudo dynamic testing." *Earthquake Engineering & Structural Dynamics*, 21(1): 79-92.
- Nakashima, M. (2001). "Development, potential, and limitations of real-time online (pseudo-dynamic) testing," *Philosophical Transactions of the Royal Society of London*, 359 (1786): 1851-1867.

- Park, K., and Medina, R.A. (2007) "Conceptual Seismic Design of Regular Frames Based on the Concept of Uniform Damage," *ASCE Journal of Structural Engineering*, 133(7), 945-955.
- Sankaranarayanan, R., and Medina, R.A. (2007). "Acceleration Response Modification Factors for Nonstructural Components Attached to Inelastic Moment-Resisting Frame Structures," *Earthquake Engineering and Structural Dynamics*, 36(14), 2189-2210.
- Sankaranarayanan, R. and Medina, R.A. (2008). "Statistical Models for a Proposed Acceleration-response Modification Factor for Nonstructural Components Attached to Inelastic Structures." Proceedings of the 14th World Conference on Earthquake Engineering, 14WCEE, Beijing, China, Paper Code 2013, October 12 -17.
- Serres, J.L. (2008). "Dynamic Characterization of a Pneumatic Muscle Actuator and Its Application to a Resistive Training Device," OhioLINK ETD Center. Retrieved from http://rave.ohiolink.edu/etdc/view?acc_num=wright1227233038
- Stoica, M., Medina, R. A., and McCuen, R. H. (2007) "Improved Probabilistic Quantification of Drift Demands for Seismic Evaluation," *Structural Safety*, 29(2), 132-145.